HIGHWAY RESEARCH RECORD

Number 382

Loading History of Bridges

7 reports
prepared for the
51st Annual Meeting

Subject Area

27 Bridge Design

HIGHWAY RESEARCH BOARD
DIVISION OF ENGINEERING NATIONAL RESEARCH COUNCIL
NATIONAL ACADEMY OF SCIENCES—NATIONAL ACADEMY OF ENGINEERING

Washington, D.C. 1972

NOTICE

The studies reported herein were not undertaken under the aegis of the National Academy of Sciences or the National Research Council. The papers report research work of the authors done at the institution named by the authors. The papers were offered to the Highway Research Board of the National Research Council for publication and are published herein in the interest of the dissemination of information from research, one of the major functions of the HRB.

Before publication, each paper was reviewed by members of the HRB committee named as its sponsor and was accepted as objective, useful, and suitable for publication by NRC. The members of the committee were selected for their individual scholarly competence and judgment, with due consideration for the balance and breadth of disciplines. Responsibility for the publication of these reports rests with the sponsoring committee; however, the opinions and conclusions expressed in the reports are those of the individual authors and not necessarily those of the sponsoring committee, the HRB, or the NRC.

Although these reports are not submitted for approval to the Academy membership or to the Council of the Academy, each report is reviewed and processed according to procedures established and monitored by the Academy's Report Review Committee.

ISBN 0-309-02051-4

Price: $2.40

Available from

Highway Research Board
National Academy of Sciences
2101 Constitution Avenue, N.W.
Washington, D.C. 20418

CONTENTS

FOREWORD

The reports in this RECORD were presented at a symposium during the Annual Meeting of the Highway Research Board. They discuss the prediction of the fatigue life of bridges from stress ranges experienced under normal traffic conditions. Stress-range data were obtained during extended periods at critical points on the main load-carrying members of each particular bridge. The research reported is part of a long-term national program initiated several years ago and described in earlier reports by Galambos and Armstrong in Highway Research Record 295 and by Galambos and Heins in Highway Research Record 354.

The authors of the first 4 reports have generally used similar experimental techniques and have arrived independently at one unanimous conclusion among their other findings: None of the various bridge types studied would be expected to sustain fatigue damage at any of the selected critical stress points based on the stress ranges experienced under extended periods of normal traffic and the application of commonly accepted cumulative damage theories. Allowances were also made for the effect of anticipated increases in the volume and composition of present traffic.

Burdette and Goodpasture present findings on the ultimate static live-load capacity of 4 types of highway bridges that were loaded to yielding in a unique field experiment. Their findings will be of considerable interest to all bridge engineers, particularly those who write specifications and who heretofore have had few experimental data on the responses of typical highway structures to incremental loading up to ultimate load capacity.

Victor describes a comprehensive field study of a horizontally curved steel girder bridge. He emphasizes that significant enhancement of design and analysis techniques for this relatively new concept of bridge construction can be achieved through the evaluation of the experimental results of such field studies.

The remarks by Galambos reconciles an apparent discrepancy between the findings of these reports and the fact that fatigue failures are occurring in highway bridges from time to time, a matter of concern to bridge engineers. Galambos points out that the conclusion that fatigue damage is not likely to occur is valid for the bridges tested in the field studies reported here and is applicable to the great majority of highway bridges. At the same time, the observed fatigue damage of highway bridges has generally been on very heavily traveled urban or intercity routes indicating that future field studies of bridge-loading history should be concentrated on bridges in these areas.

—Robert F. Varney

BRIDGE STRESS-RANGE HISTORY

P. P. Christiano, L. E. Goodman, and C. N. Sun,
Department of Civil and Mineral Engineering, University of Minnesota

A computer system for monitoring stress history data and reducing them to digital form was used to estimate the effect of traffic on the fatigue life of a 3-span, continuous-stringer highway bridge. Tests were performed by using control vehicles to measure the load-carrying characteristics of the bridge. Further, extensive stress-range data on the stringers were obtained under general traffic conditions during a 97-hour period. Results indicate good correlation between the frequency distribution of stress ranges in the most severely stressed stringer at midspan and the frequency distribution of vehicles according to weight. The stress ranges produced at both midspan and the ends of the cover plates near the internal piers were found to be very small relative to the endurance limit of the structural components.

•THE USEFUL life of a highway bridge depends on many factors, among them the fatigue strength of the structural components. Because the fatigue life of a bridge depends on its loading history, the frequency distribution of stress ranges and their relation with the character of the traffic are required. The effect of stress history on the fatigue life of a highway bridge has been presented previously (1, 2). Because the effort of data reduction greatly limited the amount of information that could be considered, a computer system has been developed to monitor strain history data and reduce it to digital form (3). Although that data acquisition system has been used in a pilot study, the investigation described here is believed to represent the most extensive use of the system and the resulting accumulation of data to date (1971).

This report describes a study of collecting and evaluating data related to the response of a 3-span, compositely designed, continuous-stringer bridge subjected to both controlled and general traffic conditions. The bridge is located in the southbound lane of Interstate 35W in Bloomington, Minnesota, which is in the metropolitan area of Minneapolis and S. Paul.

The main objectives of the investigation were the measurement of the bending stresses in the stringers under controlled traffic conditions and the recording of strain-range data under general traffic conditions. The data were used to analyze the specific structural behavior of the bridge and to obtain information regarding the fatigue life of the bridge under repeated loads.

INSTRUMENTATION AND DATA ACQUISITION

The spatial distribution of stress in the bridge under controlled loading and the frequency distribution of stress ranges imposed by the general traffic were determined from strain gauge readings. The strain gauges were mounted on the stringers and diaphragms of the bridge shown in Figure 1.

Although a total of 24 strain gauges were installed, the results of only those 10 gauges on the bottom flanges of the stringers are reported here; a detailed discussion of the behavior of all gauges is contained elsewhere (4). A gauge was placed on each of the 5 stringers at midspan (section A-A) and at a location in the center span, 4 in. from the ends of the tapered cover plates (section B-B).

Two basically different types of instrumentation were employed during this investigation. The specific type of instrumentation depended on whether strain ranges under actual traffic conditions or strains under controlled loading were being recorded. The

system for obtaining a record of the structural behavior under controlled loading comprised oscillographs.

The system for measuring the frequencies and magnitudes of strain-range occurrences is owned and operated by the Federal Highway Administration and is described in detail elsewhere (1). Basically, the system consists of Wheatstone bridge completion modules, amplifiers, an analog-to-digital converter, a digital computer, and a teletype machine. The complete system is housed in an environmentally controlled trailer. The computer is programmed to record the frequency and magnitude of a "maximum" strain range, that is, the maximum difference in strain caused by the passage of a single vehicle. As many as 10 strain gauges are read through separate channels, each of which is programmed for 10 individual strain levels. As a vehicle encounters the bridge, the system records the strain at a sampling rate as great as 200 per second and retains the maximum value until a minimum negative (i.e., below a 0 level) value is obtained. The algebraic difference of those 2 readings constitutes a maximum strain range. The system then begins a search for a new maximum strain and an associated strain range. The threshold level is placed at a certain positive strain level so that small strain ranges caused by the passage of light vehicles will not be recorded. In this study the threshold level was set at 15×10^{-6} in./in. The 0 level may be adjusted to separate the temperature effects from those caused by the live load. The 10 gauges on the stringers were recorded with this instrumentation and monitored strain-range data produced by actual traffic for the evaluation of possible fatigue damage.

The acquisition of strain-range data was begun at the beginning of the second week of October 1969 and was maintained continually for 97 hours. The data were accumulated and automatically printed on an hourly basis; the printout time was 4 minutes, during which no data were recorded. During the 97-hour period, truck traffic was counted and classified so that the traffic type with the magnitudes and frequencies of strain ranges could be correlated. During selected time intervals, samples from the truck traffic were weighed at a weigh station located approximately 8 miles south of the bridge. Unfortunately, much of the traffic left the highway before encountering the weigh station. From the weigh-station information, however, an estimate could be made with regard to the general distribution of vehicular loads.

The controlled tests were conducted by using 2 trucks (H20 and HS20) owned and operated by the Minnesota Department of Highways. The trucks encountered the bridge either separately or, in some cases, simultaneously, and the response of the gauges was recorded. The purpose of these tests was to measure the structural behavior of the bridge. In addition to the controlled tests, oscillograph readings were also taken (strain-range measurement continued simultaneously) to obtain some information about the actual stresses incurred under normal traffic conditions. Individual vehicles that happened to be isolated from the other traffic were classified, and their effects on the bridge were recorded. Of those vehicles, those that passed the weigh station were weighed.

CONTROLLED TESTS

The structural response under controlled conditions was determined by driving 2 vehicles, located at various lateral positions, across the bridge at various speeds. The H20 vehicle (double-tandem dump truck) had front and rear axle weights of 8.20 and 32.20 kips respectively; front-to-rear axle spacings were 13 ft 10 in. and 4 ft 2 in. The HS20 vehicle (5-axle semitrailer) had front-to-rear axle loads of 6.14, 32.00, and 32.16 kips; front-to-rear axle spacing was 10 ft, 4 ft, 10 ft 3 in., and 4 ft.

Test runs were made at approximately 3 speeds: 5, 25, and 40 mph. Three primary lateral vehicle positions were considered. In the first case each truck's right wheels ran a few inches from the right lane curb, and in the second case each truck was centered in the right lane. In both cases only one truck at a time was on the bridge. In the third case, both vehicles crossed the bridge simultaneously; the HS20 vehicle was centered in the right lane, and the H20 vehicle in the left lane.

Figure 1. Plan, elevation, cross section, and location of strain gauges.

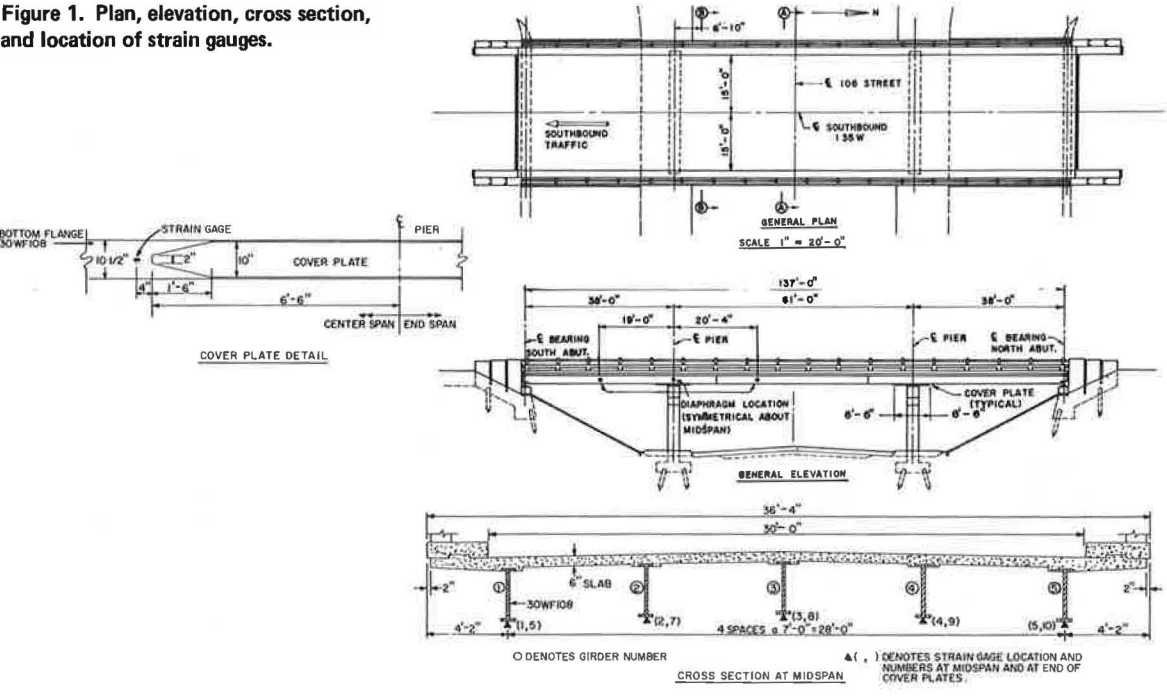

Figure 2. Positive bending stresses at midspan under controlled loading.

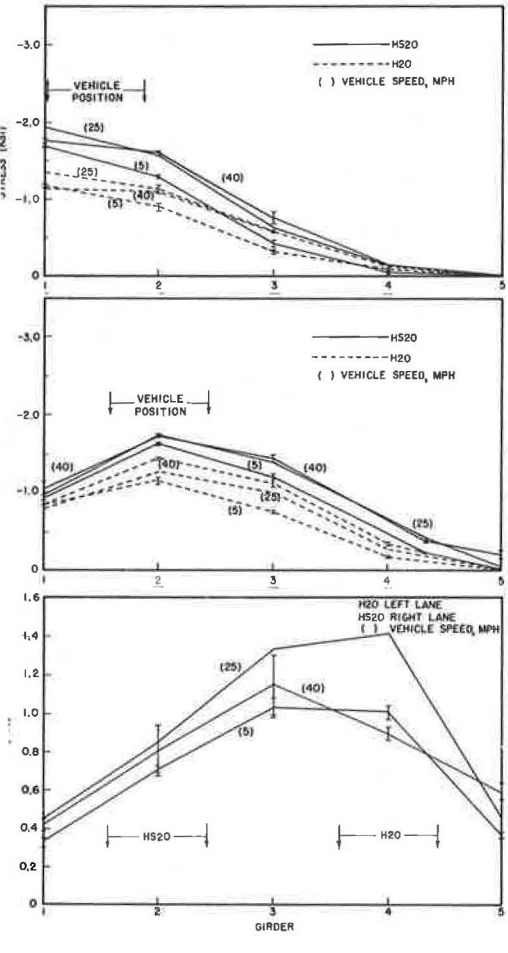

Figure 3. Negative bending stresses at ends of cover plates under controlled loading.

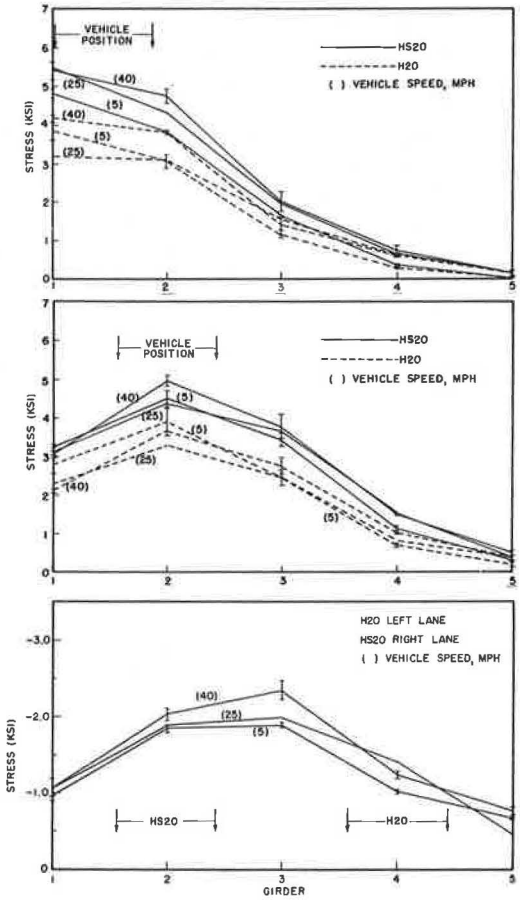

The tests involving each of the 3 primary positions were performed twice at both the crawl speed (5 mph) and the fastest speed (40 mph). Because of increasingly heavy traffic, only one set of tests was made at the intermediate speed (25 mph).

BENDING STRESSES

Midspan

Figure 2 shows the magnitudes of the bending stresses in each girder at midspan for each of the 5 vehicle positions and 3 speeds. When either vehicle ran next to the right lane curb, the greatest stress was incurred in girders 1 and 2. Girder 1 experienced, on an average, approximately 15 percent more stress than did girder 2. Furthermore, the magnitudes of the stresses in girder 3 were about 30 percent of those in girder 1. Girders 4 and 5 carried very little load in this case. The values of stresses in girder 1 ranged from 4.8 to 5.5 ksi under HS20 loading at 5 and 25 mph. Because the tests run at 25 mph were made only once, no indication of repeatability could be obtained in these cases. For both the H20 and HS20 runs, the impact factors associated with 40 mph in girders 1 through 3 were approximately 1.1, 1.2, and 1.2 respectively. These factors generally compare favorably with the results of other tests (1, 5) and with the value of 1.27 predicted by the ASSHO formula.

Figure 2 also shows the stresses incurred under a load centered in the right traffic lane. The impact factors for girders 2 and 3 are somewhat less than those indicated in the previous case. Although girder 2 assumes the greatest stress (4.4 to 5.0 ksi for HS20 loading and 3.3 to 3.9 ksi for H20 loading), girder 3 assumes more stress (3.4 to 3.8 ksi and 2.4 to 2.8 ksi) in this loading condition than in that of the curb loading. Girder 1, however, is less heavily stressed (3.0 to 3.2 ksi and 2.1 to 2.8 ksi) than girder 3 in this case or than girder 1 itself in the previous case. The maximum stress (5.5 ksi) in girder 1 under curb loading is greater than the maximum stress (5.0 ksi) in girder 2 under the right-lane loading, which compares favorably with results obtained for a type of simple-span bridge (6). Additional tests with the load located in the left lane showed the structure to behave in a symmetrical manner.

The effects of loading both lanes simultaneously reveal several interesting features. For the 3 most heavily stressed girders (1, 2, and 3), the stresses incurred at the crawl speed are essentially the same or even slightly greater than the corresponding stresses experienced under vehicular speeds of 25 mph. Of more significance, however, is that at the crawl speed the stresses measured in every girder are almost precisely those than would be obtained by superposition of the individual loadings described tn the preceding case (loads centered in right lane). The structure behaves linearly (i.e., superposition of loads applies), therefore, under static loading. However, if a similar study is made of the stresses incurred at vehicular speeds of 40 mph, it is found that the actual combination of loads yields considerably less stress (about 15 percent less) than that predicted by superposition. It may be concluded, therefore, that the impact factor is less for the combined tests than for those where the vehicles cross the bridge separately.

Ends of Cover Plates

Figure 3 shows the magnitudes of the negative bending stresses at the end of the cover plate in each girder for each vehicle position and speed. For loading along the right curb and in the center of the right lane, the most severe negative stresses are produced by the HS20 loading. The most heavily stressed girder for the case of the load centered in the right lane is girder 2; for the case of the curb loading, the negative stresses in girder 2 are slightly less than those in girder 1. The negative stresses at the ends of the cover plates were approximately 50 percent greater than the positive stresses at this section. Those negative stresses were, however, between 50 and 70 percent less than the positive stresses measured at the midspan.

STRESSES INCURRED UNDER SAMPLE TRAFFIC

For one 6-hour interval, during which the bridge was subjected to general traffic conditions, stress measurements were obtained from the passage of selected

commercial vehicles. A vehicle was chosen for this part of the study if it was sufficiently isolated from the rest of the traffic so that it alone crossed the bridge during the time that strains were measured.

Most of the commercial vehicles that crossed the bridge during the 6-hour period left the highway before encountering the weigh station; therefore, stresses could not be directly related to vehicular gross weight. Generally, higher stresses were produced by the larger classes of vehicles than by the smaller trucks. Of significance is that, in all but 1 of the 38 cases observed, girder 2 experienced the largest stress at midspan. The maximum positive bending stress incurred by girder 2 was 3.94 ksi. Only in the case where a truck crossed the bridge in the left traffic lane was the greatest stress (4.03 ksi) produced in girder 5; this was the only case where bending stress in a girder exceeded 4.00 ksi. As may be expected, the negative bending stresses at midspan were significantly less than the positive stresses.

The bending stresses at the ends of the cover plates were generally less than those at midspan. The maximum negative stress (-1.59 ksi) at the end of a cover plate occurred in girder 2. The maximum positive stress was 1.32 ksi; however, this stress is considerably larger than the average positive stress at the ends of the cover plates.

The largest stress ranges (algebraic difference between positive and negative stresses) usually occurred in girder 2. In that member the maximum stress ranges were 4.46 and 2.78 ksi at the midspan and the end of the cover plate respectively.

At midspan the maximum positive stress (4.62 ksi) produced by the HS20 vehicle occurred in girder 1; when this load was located in the center of the right lane, the maximum stress (4.94 ksi) occurred in girder 2. When both control vehicles crossed tha bridge simultaneously, the maximum stress, 6.22 ksi, was produced in girder 3. The maximum positive and negative stresses produced at the ends of the cover plates under HS20 loading were 1.41 and -1.94 ksi respectively; combined loading produced maximum stresses of 1.41 and -2.47 ksi. In all cases the stresses incurred under general selected traffic were considerably less than those produced in the controlled tests.

EFFECT OF TRAFFIC ON STRESS RANGES

A summary of the stress ranges computed from strain-range data and recorded for 97 one-hour periods is given in Table 1. Gauges 1 through 5 correspond to those placed at midspan (Fig. 1), and gauges 6 through 10 are those at the ends of the cover plates and are in the same order as the first 5 gauges. The stress ranges for each gauge are divided into 9 increments designated in units of ksi.

With the exception of gauge 5, all the gauges at midspan experienced comparable total numbers of stress-range occurrences. This may be interpreted to mean that with the passage of a single vehicle nearly the same number of stress-range values (i.e., the number of recorded peaks and valleys) occurs in each girder. Occurrences in the 2 right-lane girders (1 and 2) were approximately 16 and 6 percent more respectively than the total average occurrences in the 4 girders; occurrences in the other girders (3 and 4) were about 14 and 10 percent less than the average. The comparison of the total number of occurrences among the 5 girders gives some indication of the distribution of loading across the bridge at midspan. That the fifth girder experienced so many fewer stress-range events seems to indicate that the outer girders are effective only when the loading is in the lane corresponding to that member.

Although the total numbers of stress-range events among the various structural members may be of similar magnitudes, the distribution of these events relative to particular stress ranges may be distinctly different. Figures 4 and 5 show the percentage frequency distribution of strain-range occurrences for each gauge. The values corresponding to stress-range events between 0 and 2.85 ksi (i.e., the first 4 increments of stress ranges) were, for gauges 1, 3, 4, and 5 respectively 98.8, 95.0, 98.5, and 97.8; for the second girder (gauge 2) the corresponding value was 90.8. This comparison indicates that the second girder experiences 9.2 percent of its stress-range events over the 2.85-ksi range, whereas the other gauges experience considerably fewer events above

Table 1. Stress-range occurrences for 10 gauges.

Gauge	0.45 to 1.05 ksi	1.05 to 1.65 ksi	1.65 to 2.25 ksi	2.25 to 2.85 ksi	2.85 to 3.45 ksi	3.45 to 4.05 ksi	4.05 to 4.65 ksi	4.65 to 5.25 ksi	5.25 to 5.85 ksi	Total
1	6,901	10,679	3,375	1,201	241	18	5	0	0	22,420
2	9,816	5,125	2,698	1,090	718	728	349	100	10	20,634
3	7,434	5,352	1,897	1,130	651	154	23	5	1	16,647
4	12,756	3,277	866	337	99	60	54	37	11	17,497
5	2,840	2,947	1,282	410	122	42	3	1	0	7,647
6	290	101	19	5	3	0	0	0	0	418
7	2,252	1,808	1,016	734	53	3	0	0	0	5,866
8	910	933	400	59	19	0	0	0	0	2,322
9	597	685	244	69	5	0	0	0	0	1,600
10	155	28	7	3	1	0	0	0	0	194

Figure 4. Stress-range occurrences at midspan.

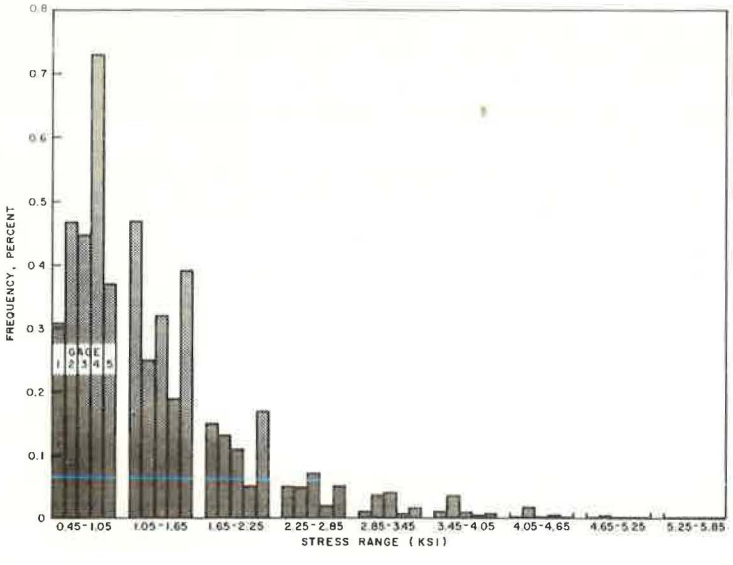

Figure 5. Stress-range occurrences at ends of cover plates.

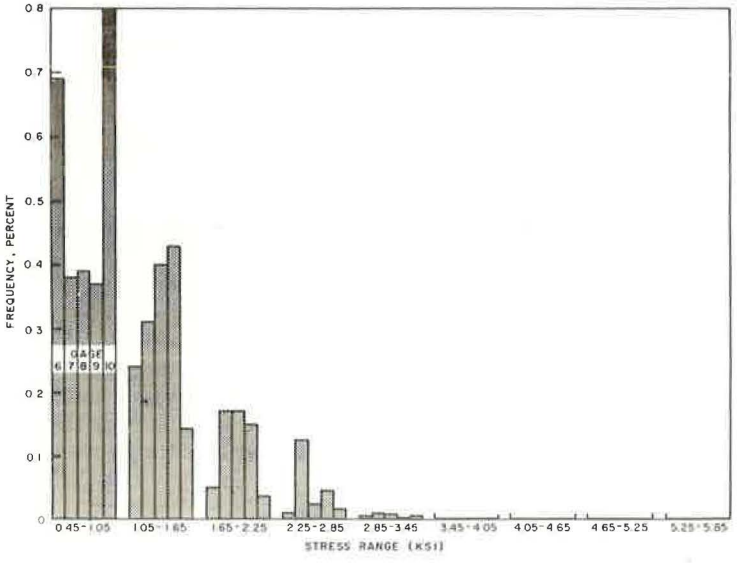

Table 2. Average 24-hour traffic volumes.

Vehicle Type[a]	24-Hour Weekday Average	Average Annual Daily Volumes 1969	1975
0	14,967	15,992	23,416
1	791	549	676
2	689	592	912
3	65	56	58
4	149	100	133
5	857	661	1,089
6	170	149	217
Total	17,688	18,099	26,501

[a] 0 = passenger cars and 4-tire trucks; 1 = single unit, 2 axle, 6-tire trucks; 2 = single unit, 3-axle trucks; 3 = truck tractor-semitrailers, 3 axle; 4 = truck tractor-semitrailers, 4 axle; 5 = truck tractor-semitrailers, 5 axle; and 6 = buses and trucks with trailers.

this range. Furthermore, in the range above 3.45 ksi the second girder experiences 5.8 percent of the total occurrences; the next highest percentage above this range is 1.1 percent in girder 3. Although in girder 2 the percentage occurrence above 3.45 ksi may be large compared with that in the other girders both at midspan and at the ends of the cover plates, it is still too small to affect the fatigue life of the member.

The total number of stress-range occurrences at the end of the cover plate in each girder was considerably less than that at midspan. Again, the gauge on the second girder recorded the most stress events (5,866) and the highest percentage (28.4 percent) relative to the total number of events in that girder at midspan. Gauges 9 and 10 recorded about a third fewer events than gauges 6 and 7 because there were statistically fewer vehicles crossing in the left lane than in the right lane.

For girders 1 and 5, the cumulative percentage stress-range occurrences less than 1.05 ksi were 30.8 and 37.1 respectively at midspan and 69.4 and 79.9 respectively at the cover plates. Further, in the range less than 1.65 ksi the cumulative percentages of occurrences were 78.4 and 75.7 at midspan and 93.5 and 94.5 at the cover plates. These comparisons indicate a symmetrical structural action about the center girder. It is again emphasized, however, that, because of the loading pattern and varying structural behavior along the length of the bridge, the bases for these percentages are distinctly different. A similar comparison may be made of the behavior of girders 2 and 4.

The cumulative percentage stress-range occurrence above 2.85 ksi in girder 2 (gauge 7) was 1.0 percent. Although this percentage is much smaller than that (9.2 percent) in the same girder at midspan, the lower fatigue life of the cover plate connections makes such a location the more critical one. As shown subsequently, although the fatigue life of the connection is less than that of the midspan section, it is not critical with regard to the useful life of the bridge. Such behavior was previously demonstrated in a similar study (1).

VEHICLE COUNT AND CLASSIFICATION

A nearly continuous traffic count and classification were made at the bridge site and tabulated hourly. Table 2 gives traffic counts for an average 24-hour interval; then data were supplied by the Minnesota Department of Highways. The second column represents an average based on the 97-hour interval during which a traffic count was conducted. Corrected average annual daily volumes to account for seasonal variation are also given for 1969 and for 1975.

FREQUENCY DISTRIBUTIONS OF VEHICLE TYPES AND GROSS WEIGHTS

Through a regression analysis a relation may be obtained between the number of occurrences in each stress range of a gauge and each type of vehicle crossing the bridge. Such an analysis fits the best (in the least squares sense) hyperplane to the acquired data of hourly strain-range events and hourly classified vehicle counts. However, the period of time over which data were obtained was too short to yield reliable results, and an alternative approximate method was used.

During a 32-hour period a total of 427 vehicles that encountered the weigh station were weighed. The number of vehicles that were weighed did not include all the vehicles that crossed the bridge because normally many trucks leave the highway before reaching the weigh station. Further, of those vehicles that did encounter the weigh station, the larger vehicles were weighed but many smaller ones were permitted to pass by. Therefore, the frequency distribution of vehicle gross weights established at the weigh station is intentionally biased toward the larger trucks. The percentage distribution of all vehicles weighed by type in each weight range is given in Table 3. The fraction of each vehicle type in each weight category is given in Table 4. These fractional values are further used to estimate the frequency distribution of vehicle

Table 3. Percentage distribution of all vehicles by type and weight category.

Vehicle Weight (kip)	Total Vehicles		Percentage Distribution by Type						
	Number	Percent	1	2	3	4	5	6	7
0-10	30	7.0	3.3	3.5	–	0.2	–	–	–
10-20	54	12.6	0.2	8.0	2.8	0.2	0.7	0.2	0.5
20-30	107	25.1	–	4.0	0.9	1.6	3.8	14.3	0.5
30-40	63	14.8	–	–	1.2	1.4	2.8	9.4	–
40-50	43	10.2	–	–	1.2	1.2	2.6	5.2	–
50-60	32	7.5	–	–	–	0.2	1.4	5.9	–
60-70	34	8.0	–	–	–	–	0.5	7.5	–
70-80	64	15.0	–	–	–	–	0.2	14.8	–
Total Percent		100.0	3.5	15.5	6.1	4.8	12.0	57.3	1.0
Number	427		15	66	26	21	51	244	4
Avg weight, kip			6.16	14.88	27.04	31.72	37.36	49.48	19.70

Note: Discrepancy in percentages total due to rounding.

Table 4. Fraction distribution of each vehicle type by weight category.

Vehicle Weight (kip)	Type 1	Type 2	Type 3	Type 4	Type 5	Type 6	Type 7
0-10	0.933	0.227	-	0.048	-	-	-
10-20	0.067	0.515	0.462	0.048	0.059	0.004	0.500
20-30	-	0.258	0.154	0.333	0.314	0.250	0.500
30-40	-	-	0.192	0.286	0.235	0.164	-
40-50	-	-	0.192	0.238	0.216	0.090	-
50-60	-	-	-	0.048	0.118	0.102	-
60-70	-	-	-	-	0.039	0.131	-
70-80	-	-	-	-	0.020	0.258	-
Total	1.000	1.000	1.000	1.000	1.000	1.000	1.000

Figure 6. Distribution of vehicles by type at bridge site and weigh station.

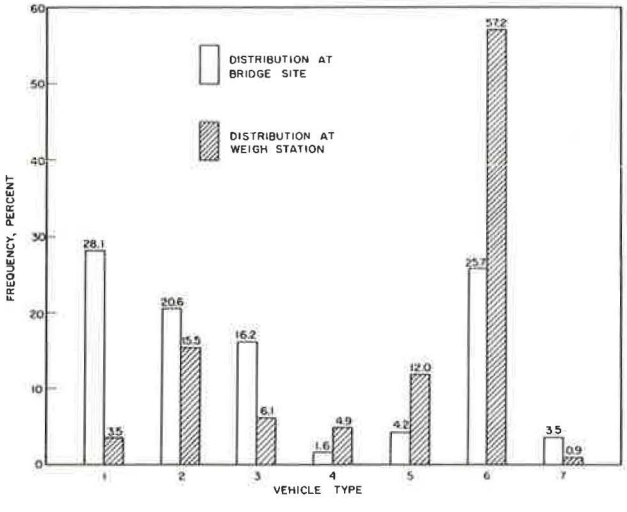

gross weights at the bridge site. Vehicle types in these tables and subsequent figures are as follows:

Vehicle	Code Number
Light truck, 2-axle, single-tire	1
Single-unit, 2-axle truck	2
Single-unit, 3- to 4-axle truck	3
Truck tractor-semitrailer, 3-axle	4
Truck tractor-semitrailer, 4-axle	5
Truck tractor-semitrailer, 5- to 6-axle	6
Truck with trailer	7

Figure 6 shows a comparison between frequency distribution at the weigh station and at the bridge site according to vehicle type. The frequency distribution by vehicle type at the bridge site differs considerably from that at the weigh station. Because of the bias sampling, there was at the weigh station a smaller percentage of lighter (single unit) trucks and a greater percentage of heavier (truck-semitrailer) vehicles.

An estimate was made of the frequency distribution at the bridge site according to vehicle gross weight by converting the distribution according to vehicle type 5 with the use of the fractional values given in Table 4. The distribution, according to vehicle gross weight and the stress-range distribution at the midspan of girder 2 (from Fig. 3), is shown in Figure 7. Except for the lowest and highest ranges, good correlation exists between the frequency distributions of vehicle gross weights and stress ranges. Therefore, it appears that the behavior of the most heavily stressed member (girder 2) at midspan is very closely related to the frequency and magnitude of the loading. This comparison is essentially a simplified regression analysis that is useful when sufficient data for a more rigorous analysis are unavailable. A comparison of stress-range distribution in a member other than girder 2 with the vehicle gross weight distribution shows poorer correlation. Girder 2 experiences the broadest distribution and the greatest number of stress-range occurrences; therefore, this member should serve as the best indicator in such a comparison.

FATIGUE LIFE ANALYSIS

The fatigue life of a structure is affected by a combination of many factors. The most important considerations are loading history and loading expectation, fatigue strength and structural details, stress range and mean stress, and temperature variation and corrosion.

Although neither loading history nor future loading is known with certainty, they may be estimated from data related to the current pattern of dynamic loading. These data specify the frequencies and magnitudes of stress ranges corresponding to traffic volume. As stated previously, girder 2 experienced the greatest frequencies and magnitudes of stress ranges. Table 5 gives the number of occurrences of the live load stress ranges in girder 2 for the 97-hour test period. These data are used to obtain current (1969) annual and future (1975) frequency estimates. Because the method of collecting strain-range data grouped the data in discrete intervals, the stress ranges shown in the following represent the mean value in each interval. For example, the stress range 0.45 to 1.05 ksi is replaced by 0.75 ksi.

The fatigue strength of any structural component depends on the mean stress level as well as the stress range. If temperature effects are ignored, the minimum stress at any point in the structure may be taken as that produced by the dead load. If no composite action is assumed to exist in positive moment zones, the dead-load stresses in an inner girder at midspan and at the end of the cover plate are 5.39 ksi and 2.56 ksi respectively. Because of the uncertainty of composite action, these stress values were used to develop fatigue curves.

The fatigue curves may be developed with data corresponding to test specimens subjected to zero-to-tension loading; they indicate the number of cycles at a given stress

Figure 7. Distribution of vehicle gross weights and stress ranges in girder 2.

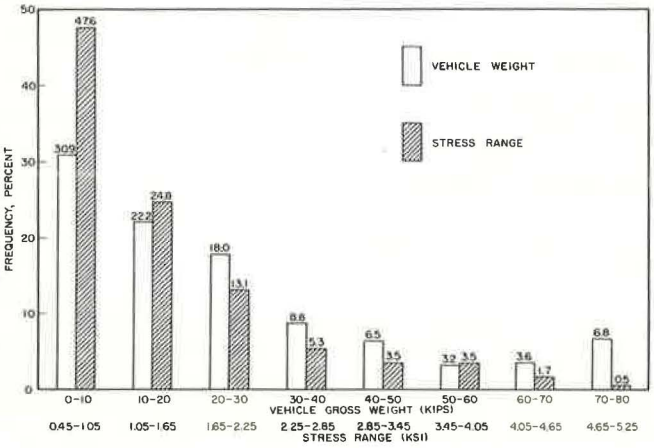

Figure 8. Fatigue curve for rolled beam with partial-length-tapered end cover plate.

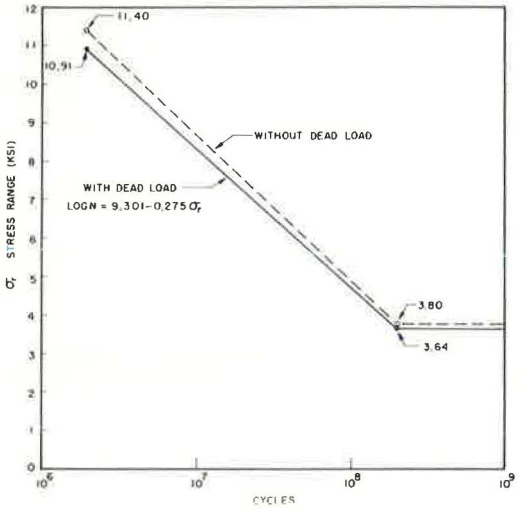

Table 5. Stress-range occurrences in girder 2.

Stress Range (ksi)	Occurrences at Midspan			Occurrences at End of Cover Plate		
		Annual Estimate ($\times 10^6$)			Annual Estimate ($\times 10^6$)	
	97-Hour	1969	1975	97-Hour	1969	1975
0.75	9,816	0.866	1.307	2,252	0.203	0.300
1.35	5,125	0.463	0.683	1,808	0.162	0.241
1.95	2,698	0.244	0.359	1,016	0.092	0.135
2.55	1,090	0.098	0.145	734	0.066	0.098
3.15	718	0.065	0.096	53	0.005	0.007
3.75	728	0.066	0.097	3	0.0003	0.0004
4.35	349	0.032	0.046	0	0	0
4.95	100	0.009	0.013	0	0	0
5.55	10	0.001	0.001	0	0	0

range required to bring the specimens to failure, Fatigue curves were constructed for the points at midspan and at the end of the cover plate. The fatigue curve for a structural element may be developed by first obtaining the fatigue strength at 2×10^6 cycles and then by assuming that the fatigue strength at 200×10^6 cycles is equal to a third of this value (7). Within these 2 limits a linear relationship is assumed between the stress range and the logarithm of the number of cycles.

The fatigue curves shown in Figure 8, corresponding to the end of the cover plate, were constructed by using data related to fatigue strength of flexural members with partial-length-tapered end cover plates welded all the way around (8, 9). The fatigue strength at 2×10^6 cycles, neglecting the effect of dead-load stress, is given as 11.4 ksi. Using the modified Goodman law and assuming an ultimate strength of 60 ksi give 10.9 ksi as the fatigue strength accounting for dead-load stress. The endurance limit, assuming a dead-load stress of 2.56 ksi, is 3.64 ksi. Because the only stress range in girder 2 higher than this limit was 3.75 ksi and occurred only 3 times during the 97-hour test period, the fatigue life at the end of the cover plate is about 7×10^6 years.

In the same manner the fatigue curves corresponding to the midspan of the girder were obtained from data for ASTM A-7 steel (8). If the effect of the mean stress is neglected, the fatigue strength at 2×10^6 cycles is 31.2 ksi. The fatigue strength is 24.8 ksi if dead load is taken into account. The endurance limit for a plain rolled beam of A-7 steel with a minimum stress of 5.39 ksi is 9.47 ksi; and, because the maximum recorded stress range is 5.55 ksi, it may be concluded that at midspan (the point of maximum stress) there exists almost an unlimited fatigue life.

CONCLUSIONS

The primary objectives of this study were to collect strain-range data on a specific highway bridge of a common type, to determine the implications of those data for the fatigue life of the bridge, and to measure stresses produced in the structure by actual traffic. Some conclusions drawn from the results of this investigation are as follows:

1. The greatest number of stress-range events produced by general traffic during a 97-hour period occurred at midspan in the external stringer under the right traffic lane (girder 1). The most severely stressed member at midspan was girder 2, the stringer intermediate between the right external stringer and the centerline stringer. Girder 2 experienced nearly as many stress-range events as did girder 1 and had more events occurring in the higher stress ranges (up to 5.55 ksi).
2. The number of stress-range events occurring in the most heavily stressed member (girder 2) at the end of the cover plate was approximately one-fourth that produced at midspan. Further, a negligible percentage of stress-range events occurred above 3.45 ksi, and no events greater than 4.05 ksi were produced at this section.
3. In only one case among those vehicles from the general traffic that were recorded individually was the peak midspan live load bending stress as great as 4.0 ksi. At the end of the cover plate on girder 2, the most heavily stressed girder, the maximum negative live-load stress under general traffic was -1.59 ksi. The stresses produced by the general traffic were considerably less than those produced by either the H20 or HS20 control vehicles. The HS20 control vehicle produced a midspan bending stress of 5.62 ksi and a stress of -2.47 ksi at the end of the cover plate on girder 2.
4. The stress ranges produced at both the midspan and the ends of the cover plates are very small relative to the endurance limit of the structural components. It may be concluded that the effect of traffic volume similar to that currently encountered is insignificant with regard to the fatigue life of the longitudinal stringers.
5. Good correlation exists between the behavior of the most heavily stressed member (girder 2) in terms of frequency distribution of stress-range occurrences and the estimated frequency distribution of vehicle gross weights at the bridge site.

ACKNOWLEDGMENTS

The authors gratefully acknowledge the support and cooperation of the Minnesota Department of Highways and the Federal Highway Administration. The advice and

assistance of Keith Benthin and Charles Galambos of those agencies are appreciated. The opinions, findings, and conclusions expressed in this publication are those of the authors and not necessarily those of the department or administration.

REFERENCES

1. Cudney, G. R. The Effects of Loadings on Bridge Life. Michigan Department of State Highways, Res. Rept. R-638.
2. Cudney, G. R. Stress Histories of Highway Bridges. Jour. Struct. Div., Proc. ASCE, Vol. 94, No. ST12, Proc. Paper 6289, Dec. 1968.
3. Galambos, C. F., and Armstrong, W. L. Acquisition of Loading History Data on Highway Bridges. Public Roads, Vol. 35, No. 8, June 1969.
4. Christiano, P., Goodman, L. E., and Sun, C. Bridge Stress Range History and Diaphragm Stiffening Investigation. Rept. to the Minnesota Department of Highways, June 1970.
5. The AASHO Road Test: Report 4—Bridge Research. HRB Spec. Rept. 61D, 1962.
6. Bramer, C. R., et al. The Effectiveness of Diaphragms in Steel Stringer Bridges. Highway Research Program, North Carolina State Univ., Final Rept. of Proj. ERD-110-J.
7. Maximum Desirable Dimensions and Weights of Vehicles Operated on the Federal Aid System. 88th Congress, 2nd Session, Aug. 19, 1964, U.S. Govt. Printing Office, Washington, D.C., House Doc. 354.
8. Munse, W. H., and Stallmeyer, J. E. Fatigue in Welded Beams and Girders. HRB Bull. 315, 1962, pp. 45-62.
9. Wilson, W. M. Flexural Fatigue Strength of Steel Beams. Eng. Exp. Station, Univ. of Illinois, Bull. 377, 1948.

FATIGUE LIFE OF BRIDGES UNDER REPEATED HIGHWAY LOADINGS

Terry R. Douglas, Department of Civil Engineering, University of Alabama

An investigation was made to determine cumulative effects of vehicle loadings on the useful life of steel-stringer highway bridges typical of those encountered on heavily traveled routes in Alabama. Three typical steel-stringer bridges were selected for strain-gauge instrumentation and data collection to obtain their in-service stress histories. Strain-event data were collected at critical points on the steel stringers of each bridge until a representative 24-hour around-the-clock sample was obtained. Truck counts and classifications were made during the 24 hours of sampling to estimate the annual volume of trucks producing significant stresses in the steel stringers and to establish truck-type frequency distributions at each bridge. Fatigue curves were developed for the steel stringers and were used in conjunction with the stress histories and currently accepted fatigue concepts to estimate the fatigue life of each bridge. Results indicated that the bridges were not in present danger of fatigue failure. However, this conclusion is limited to the 3 bridges investigated and the interpretation of the cumulative effects of the stress events recorded at each bridge.

•THIS REPORT is a study of cumulative effects of vehicle loadings on the useful life of steel-stringer highway bridges typical of those encountered on heavily traveled highways in Alabama. It is directed toward the experimental determination and interpretarion of the ranges and frequencies of the dynamic live-load stresses produced in the steel stringers of 3 such bridges under normal traffic conditions during a typical 24-hour period at each location.

The main objectives of this investigation were to (a) determine the frequencies of various levels of stress at several selected critical points on the steel stringers of each bridge; (b) relate the spectrum of truck types to the spectrum of dynamic live-load stresses produced at selected critical points on the steel stringers of each bridge; and (c) correlate the dynamic live-load stress events produced at selected critical points by normal truck loadings with accepted fatigue concepts for predicting the fatigue life of each bridge.

Each bridge is located on a 4-lane, divided highway carrying a traffic volume in each direction of 5,000 to 7,500 vehicles per day including 750 to 1,000 trucks other than panels and pickups. Results from loadometer studies on these routes indicated that approximately 10 percent of all trucks have loads heavier than those recommended by AASHO. Approximately 19 percent of the single-unit, 3-axle trucks were found to be overloaded; furthermore, about 6 percent of those were overloaded by 50 percent or more.

With continually increasing sizes, weights, and volumes of heavy trucks in highway traffic, the Bridge Bureau of the Alabama Highway Department has been increasingly concerned about the increased live-load dynamic stresses resulting from such traffic and the probable effects such stresses have on fatigue life of its bridges, particularly old bridges. This concern about the fatigue life of bridges is shared by all other highway departments and the Federal Highway Administration. This study was aimed at determining whether the 3 bridges investigated, which are typical of most steel girder designs, were subject to structural distress from fatigue stresses in the rolled steel girders.

TEST BRIDGES

The 3 bridges selected for investigation had steel-stringer spans with diaphragms or crossbeams connecting the individual stringers at the ends of the span and at intermediate points. Two of the bridges were simple-beam spans, and the third was the first span of a 3-span continuous bridge. Each bridge had a reinforced concrete deck and was designed for AASHO HS20-44 loading. The 2 simple spans were composite and the 3-span continuous was noncomposite construction. Each bridge had partial-length-tapered end cover plates with continuous fillet welds all around. The test bridge number, location, type, and span length are given in Table 1.

INSTRUMENTATION

At each test bridge electrical resistance strain gauges were attached to the 2 steel stringers in the primary traffic lane at the points of maximum moment and at points 4 in. from the ends of the cover plates. Previous study (1) has indicated that a distance of 4 in. from the end of the cover plate is far enough so that the strain measured is not at the point of maximum stress concentration and is near enough so that measurements reflect the strain response at the end of the cover plate. All strain gauges were located immediately below the web on the outer surface of the bottom flanges of the steel girders

DATA COLLECTION

In-service stress history for each of the 3 bridges was obtained by collecting strain-event data concurrently from the 4 individual gauge locations for given time intervals, ranging from 4 to 8 hours, until a representative 24-hour around-the-clock sample was obtained. Truck counts and classifications were made at each bridge during the 24 hours of sampling to estimate the annual volume of trucks producing significant stresses in the steel stringers and to establish truck-type frequency distributions at each bridge.

Preliminary monitoring at the 4 selected critical points on each bridge indicated that panels, pickups, and automobiles caused no significant stresses at those selected points. Therefore, the representative 24-hour samples were restricted to the truck types shown in Figure 1, to buses, to tractors towing house trailers, and to any trucks not otherwise classified or excluded. Sampling of the strain events began in April 1969 and was concluded in June 1970. Samples were taken Monday through Thursday, excluding holidays, during the months of April, May, June, and July.

FREQUENCIES OF TRUCK TYPES

Frequency distributions of the 5 most common truck types as determined from the representative 24-hour sample for each bridge location are shown in Figure 2. In general, these distributions were quite similar except for some minor variations. Type III trucks were more frequent on bridge 1 than on the other bridges probably because those trucks were used in coal mine operations in the immediate vicinity. It was not unusual for this type of truck to cross the bridge 2 to 4 times daily between 8:00 and 3:00. Figure 2 shows that type 3S2 trucks were the most frequent on each bridge.

Figure 2 also shows the number of trucks counted during the representative 24-hour sample. This 24-hour count, when multiplied by 365, was used to estimate the annual truck volume causing possible significant stresses in the steel stringers.

STRAIN RESPONSE AND STRESS HISTORIES

A typical oscillograph record showing the strain response at the point of maximum moment and at the end-of-cover-plate locations of both instrumented stringers of bridge 1 is shown in Figure 3. This response was caused by the passing of a heavily loaded, type III truck traveling approximately 40 mph in the primary traffic lane of the bridge. The strain response is characterized by a single maximum value with no significant rebound strain. The oscillograph record shown in Figure 3 is typical of the several thousand strain events recorded for the test bridges. The stress range for a single event is defined as the algebraic difference between the maximum and minimum stresses.

Table 1. Description of test bridges.

Bridge	Span Length (ft)	Bridge Type	Location
1	80	Simple span, rolled beams with tapered end cover plates	Over Southern Railroad on road from Sayre to Alden
2	50	Simple span, rolled beams with tapered end cover plates	Over Warrior River on road from Kimberly to Blount County line
3	80½	First span of 3-span continuous, rolled beams with tapered end cover plates	Over Alabama River on road from Hunter Station to Prattmont

Figure 1. Truck identification and codes.

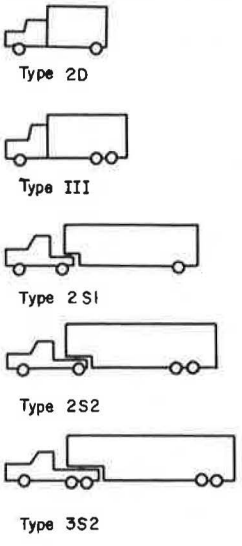

Figure 2. Distribution of 5 most common types of trucks.

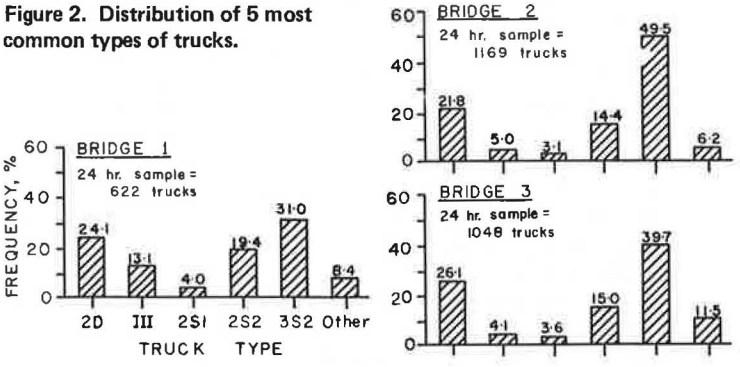

Figure 3. Typical strain or stress response of bridge 1.

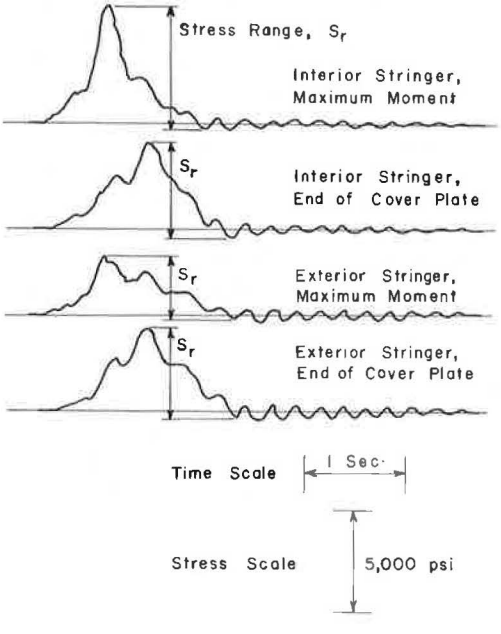

Figure 4. Distribution of stress range at end-of-cover-plate point on interior stringer.

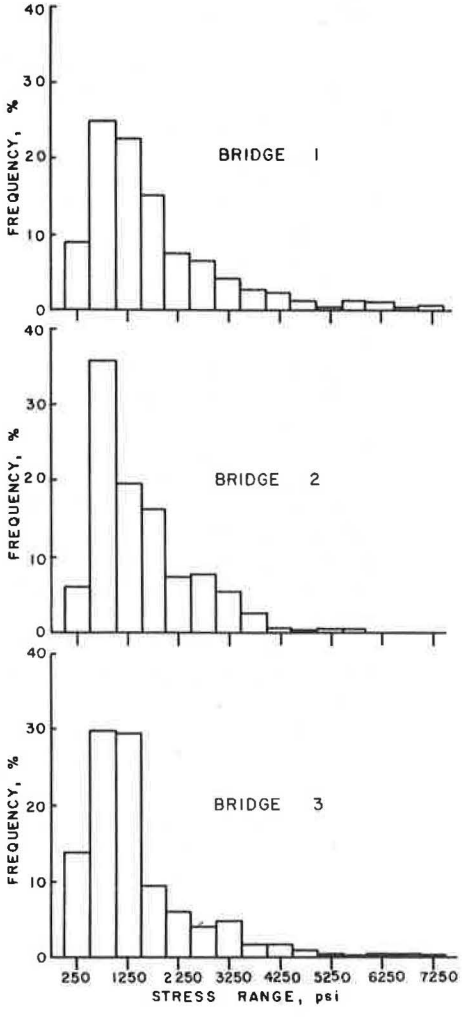

Summaries of the stress-range frequencies for the most critical point, insofar as fatigue is concerned, on each bridge are shown in Figure 4. These stress-range frequency distributions were determined from the strain events recorded during the 24-hour sampling period for each bridge.

FATIGUE CURVES

Fatigue curves presented in this report for steel beams with partial-length cover plates were developed from the Munse-Stallmeyer data (2) and the modified Goodman law (3) to establish stress-range values and their corresponsing number of cycles to failure. Munse and Stallmeyer presented test results demonstrating the effects of structural details on the fatigue behavior of welded flexural members. Included in the data for partial-length-tapered end cover plates welded all around were the stress range values at 2×10^6 cycles and 1×10^5 cycles for constant cycle zero-to-tension loading. The stress-range values at 2×10^6 cycles and 1×10^5 cycles were reported as 11,400 and 34,000 psi respectively. These data were obtained from tests conducted on A-373 steel rolled beams with partial-length-tapered end cover plates welded all around by using E7016 electrodes and manual arc welding.

The Munse-Stallmeyer fatigue data on partial-length-tapered end cover plates were obtained by constant cycle zero-to-tension tests. The minimum stress during these cyclic loading tests wes zero. In actuality, because of the weight of the bridge structure itself, there exists in the steel bridge stringers a minimum or dead-load stress of other than zero. A loading test that includes a dead load or minimum stress is referred to as a constant cycle dead load-to-tension loading test. The effect of this dead load or minimum stress for a constant fatigue life is to reduce the corresponding stress range value.

One procedure for determining the effect of a dead load or minimum stress for a constant fatigue life on the stress-range value obtained from zero-to-tension loading tests is shown in Figure 5. This procedure is known as the modified Goodman law or modified Goodman diagram. These diagrams were constructed from the basic Munse-Stallmeyer data by assuming an ultimate tensile strength of 60,000 psi. The stress-range value (3,800 psi) at 2×10^8 cycles for zero-to-tension loading ($S_{min} = 0$) was calculated as $\frac{1}{3}$ the stress-range value at 2×10^6 cycles ($S_{min} = 0$) according to House Document 354 (4). The diagrams shown in Figure 5 are plotted as straight lines in such a way that they converge on the ultimate tensile strength. As demonstrated by Grover, Gordon, and Jackson (3), this straight-line approximation of fatigue behavior at various lifetimes gives conservative values of stress range for minimum stresses below the ultimate tensile strength.

Fatigue curves shown in Figures 6 and 7 were developed for the end-of-cover-plate gauge locations only because the stresses determined at other gauge locations (at points of maximum bending moment) were well below the endurance limit of the material. These fatigue curves were developed by using 2 methods in which dead-load stresses were both neglected and considered. This procedure resulted in a total of 4 different curves describing the fatigue behavior at the end-of-cover-plate gauge locations. Dead-load stresses at the end of cover plates were estimated from bridge plans, and an average value of 7,500 psi was selected as being representative and was used in preparing the fatigue curves.

Method 1 fatigue curves (Fig. 6) were developed by assuming a linear log-log relation between stress range and cycles to failure. Method 2 fatigue curves (Fig. 7) were developed by assuming a linear relation between stress range and the logarithm of cycles to failure.

FATIGUE LIFE

The service conditions of bridges require that the steel stringers undergo many cycles of stress having many different magnitudes applied in a random manner. Miner's cumulative fatigue damage theory allows these factors to be considered when fatigue data are analyzed (5).

Figure 5. Modified Goodman diagram prepared from Munse-Stallmeyer data for partial-length-tapered end cover plates welded all around.

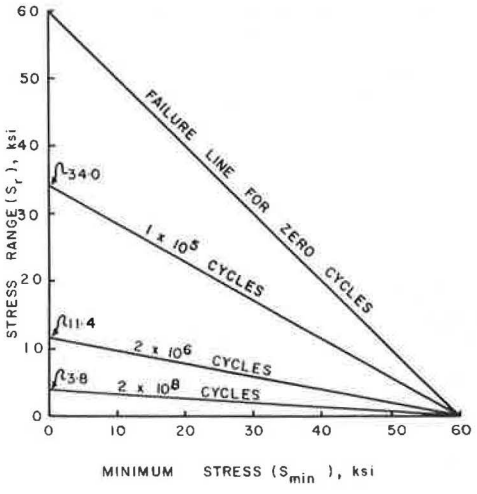

Figure 6. Method 1 fatigue curves.

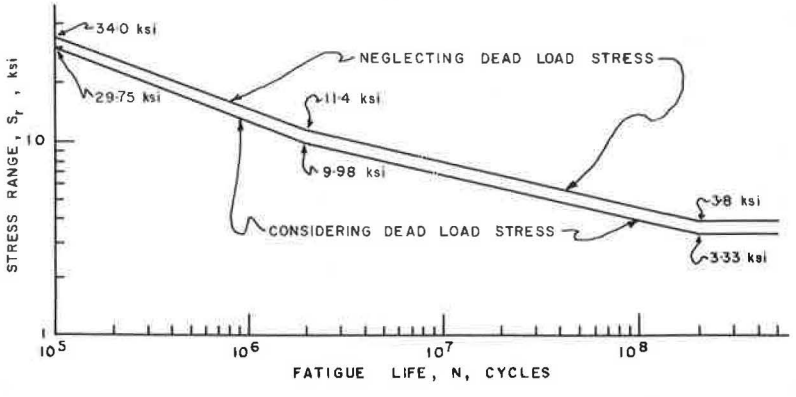

Figure 7. Method 2 fatigue curves.

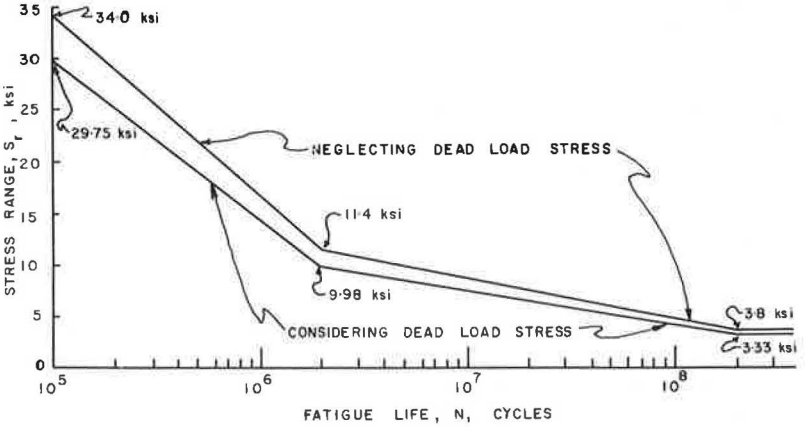

Table 2. Estimated fatigue lives and annual truck volume for test bridges.

Bridge	Annual Truck Volume	Fatigue Life Considering Dead-Load Stress (year)		Fatigue Life Neglecting Dead-Load Stress (year)	
		Method 1	Method 2	Method 1	Method 2
1	227,030	1,329	2,118	2,160	3,516
2	382,520	2,599	4,198	4,516	6,640
3	426,685	6,181	8,536	10,742	12,226

In Miner's theory it is hypothesized that, if a material is subjected to n_i cycles at a stress-range level S_i where its expected fatigue life is N_i cycles, the fractional fatigue life used up is n_i/N_i. It is further assumed that, if a material is subjected to a stress-range spectrum $S_1, S_2, \ldots, S_i, \ldots$ and if the cycles are applied $n_1, n_2, \ldots, n_i, \ldots$ times at the respective stress-range level, then fatigue failure will occur when

$$\sum_{i=1}^{k} n_i/N_i = 1$$

Miner's cumulative damage theory was used in conjunction with each of the 4 fatigue curves for determining the fatigue life of each bridge based on the stress-range frequency distribution at the end-of-cover-plate gauge location on the most highly stressed stringer. For each bridge the interior stringer was found to be most highly stressed.

Table 2 gives the predicted fatigue life of each bridge and the estimated annual truck volume causing possible significant stresses in the steel stringers (details of procedure used to determine fatigue lives and given in the Appendix.) The estimated annual truck volume, determined by multiplying the 24-hour count by 365, and the stress-range frequency distributions were assumed to be constant for the entire life of each bridge in determining the fatigue lives.

With both methods, the fatigue lives determined by considering dead-load or minimum stress were significantly less than fatigue lives determined by neglecting dead-load stress. Fatigue lives based on method 1 were less than corresponding ones based on method 2. The several fatigue lives were calculated for each bridge to emphasize the wide variations that exist depending on the particular relation assumed between stress range and cycles to failure and whether minimum stresses are considered. The large variations in fatigue life predicted by these several procedures would indicate that additional experimental work is needed for determining more rational estimates of fatigue life, thereby narrowing the range of uncertainty.

CONCLUSIONS

Only a casual inspection of the estimated fatigue lives given in Table 1 for the 3 bridges is required to see that in no case is the fatigue life less than 1,329 years, and in most cases it is considerably longer. If it is assumed that either of the procedures used for determining fatigue lives is reasonably valid, one would conclude that currently employed bridge design specifications lean heavily toward the conservative side. This conclusion, however, is necessarily limited to the 3 bridges investigated and to the critical points considered on the stringers of these bridges.

The validity of the fatigue lives given in Table 1 is limited to the applicability of the Munse-Stallmeyer data, Goodman's modified law, Miner's cumulative damage theory and the interpretations explained in the body of this report.

The Munse-Stallmeyer data were extrapolated by assuming the stress range value 2×10^8 cycles to be $\frac{1}{3}$ the stress range value at 2×10^6 cycles according to House Document 354 (4). This extrapolation was necessary because no fatigue data in this range were available.

The Munse-Stallmeyer data were restricted to stress-range values obtained from constant cycle zero-to-tension loading tests. To incorporate the effect of a constant dead-load or minimum stress on the fatigue lives, the modified Goodman law was used to modify the stress-range values obtained from constant cycle zero-to-tension loading tests.

Miner's cumulative damage theory assumes that fatigue damage is independent of the order of application of the various stress levels. In reality, bridges are subject to random loadings and hence random stresses, and the use of a fatigue damage concept neglecting this fact may not be entirely valid.

Other factors that were not considered in this study and that could significantly affect the fatigue life of the steel-stringer bridges include the effect of combined stresses, surface roughness, residual stresses, temperature ranges, creep, and corrosion. Each of these factors would tend to alter the fatigue life if their effects could be incorporated

ACKNOWLEDGMENTS

This investigation was performed in the Civil Engineering Department of the University of Alabama at Tuscaloosa under the sponsorship of the Alabama Highway Department and the Federal Highway Administration. The support, cooperation, and assistance given by these organizations is gratefully acknowledged. However, the opinions, findings, and conclusions expressed in this paper are those of the author and not necessarily those of the Alabama Highway Department or the Federal Highway Administration.

REFERENCES

1. Hulsbos, C. L., and Linger, D. A. Dynamic Tests of a Three-Span Continuous I-Beam Highway Bridge. HRB Bull. 279, 1961, pp. 18-46.
2. Munse, W. H., and Stallmeyer, J. E. Fatigue in Welded Beams and Girders. HRB Bull. 315, 1962, pp. 45-62.
3. Grover, H. J., Gordon, S. A., and Jackson, L. R. Fatigue of Metals and Structures. U.S. Govt. Printing Office, Washington, D.C., 1954.
4. Maximum Desirable Dimensions and Weights of Vehicles Operated on the Federal Aid System. 88th Congress, 2nd Session, August 19, 1964, House Doc. 354, U.S. Govt. Printing Office, Washington, D.C., pp. 143-149.
5. Miner, M. A. Cumulative Damage in Fatigue. Jour. of Applied Mechanics, Vol. 12, Sept. 1945, pp. A-159.
6. Cudney, G. R. The Effects of Loadings on Bridge Life. Highway Research Record 253, 1968, pp. 35-71.
7. Richart, F. E., Jr., and Newmark, N. M. An Hypothesis for the Determination of Cumulative Damage in Fatigue. Proc. ASTM, Vol. 48, 1949.
8. Dolan, T. J., Richart, F. E., Jr., and Work, C. E. The Influence of Fluctuations in Stress Amplitude on the Fatigue of Metals. Proc. ASTM, Vol. 49, 1949, pp. 646-682.
9. AASHO Road Test: Report 4—Bridge Research. HRB Spec. Rept. 61D, 1962.
10. Daniels, J. H., and Fisher, J. W. Fatigue Behavior of Continuous Composite Beams. Highway Research Record 253, 1968, pp. 1-20.
11. Stephenson, H. K., Noel, J. S., and Mayfield, A. D. Truck Weight Trends Related to Highway Structures. Texas Transportation Institute, Bull. 19, July 1962.
12. Galambos, C. F., and Armstrong, W. L. Loading History of Highway Bridges. Federal Highway Administration, May 1968.

APPENDIX

EXAMPLE OF PROCEDURE USED TO DETERMINE FATIGUE LIVES

This example illustrates the calculations for determining the fatigue life of bridge 1 based on the stress ranges and frequencies at the end-of-cover-plate point on the most highly stressed stringer; method 1 considering dead-load or minimum stress is used. (Method 1 provides a more conservative estimate of fatigue life than method 2.) Other fatigue lives given in Table 1 were determined in a similar manner.

1. From the proper stress-range frequency distribution (Fig. 4), determine the stress ranges and their corresponding frequencies as given in Table 3, columns 1 and 2 respectively. The estimated annual truck volume causing possible significant stresses was estimated from the 24-hour count to be 22,030.
2. Multiply each of the stress-range frequencies by the annual truck volume to determine the annual number of damage cycles at each of the stress-range levels as given in column 3 of Table 3.
3. From the proper fatigue curve (Fig. 6), determine the fatigue life at each of the stress-range values given in column 4 of Table 3.

Table 3. Fatigue life factors for bridge 1.

Stress Range (ksi)	Stress-Range Frequency (percent)	Annual Damage Cycles	Fatigue Life (10^7)	Annual Damage (10^{-3})
7.25	0.645	1,464.3	0.761	0.192
6.75	0.483	1,096.6	1.027	0.106
6.25	0.967	2,195.4	1.418	0.155
5.75	1.130	2,565.4	2.011	0.128
5.25	0.483	1,096.6	2.945	0.037
4.75	1.130	2,565.4	4.480	0.057
4.25	2.410	5,471.4	7.142	0.077
Total				0.752

4. Divide each of the annual damage cycles by the corresponding fatigue life as given in column 5 to obtain the annual damage factor at each of the stress-range values.

5. Add all the annual damage factors in column 5 to obtain the total annual damage.

The fatigue life is determined by taking the reciprocal of the total annual fatigue damage that corresponds to the fatigue life given in Table 2. For this example the total annual fatigue damage was found to be 0.752×10^{-3} or 0.000752. This means that 0.000752 represents the fractional part of the fatigue life of bridge 1 that is used up annually. Therefore, the estimated fatigue life of bridge 1 is as follows:

$$\text{Fatigue life} = 1/\text{total annual fatigue damage}$$
$$= 1/(0.752 \times 10^{-3}) = 1{,}329 \text{ years}$$

The fatigue life calculated in this example and those given in Table 2 were determined by assuming a constant annual volume of trucks causing possible significant stresses. If the annual truck volumes were to increase, there would be a corresponding decrease in the bridge fatigue lives.

If it is assumed that the annual truck traffic at the end of the bridge fatigue life is 10 times the present 227,030 and if it is further assumed that the increase is linear with time, it would mean that the average annual truck volume would be 5.5(227,030). The average total annual fatigue damage would be 5.5 times the present 0.752×10^{-3}. Based on these assumptions, therefore, the estimated fatigue life of bridge 1 would be $1/5(0.752 \times 10^{-3}) = 241$ years.

If the annual volume of truck traffic at bridge 1 were to remain constant from year to year, its estimated fatigue life by method 1 considering minimum (dead-load) stress would be 1,329 years. But if it is assumed that the annual truck traffic increases linearly with time and reaches 10 times the present volume at the end of the bridge fatigue life, the estimated fatigue life would be reduced to 241 years.

Because a tenfold increase in the annual truck traffic is not likely to be reached, it would appear that the estimated fatigue life of bridge 1 would be somewhere between 241 and 1,329 years. If perfect maintenance, no change in vehicle weights and composition of truck traffic, and a more moderate increase in such traffic are assumed, the theoretical fatigue life of bridge 1 would probably be between, say, 500 to 600 years.

COMPARISONS BETWEEN INDUCED GIRDER STRESSES AND CORRESPONDING VEHICLE WEIGHTS

Conrad P. Heins, Jr., and Ratten L. Khosa,
Department of Civil Engineering, University of Maryland

The report presents the partial results of 4 loading history field tests on 4 simple-span, cover-plated bridges in Maryland. The resulting stress-range data are compared to the stiffness of a typical girder and the corresponding vehicle gross weights. The vehicle gross-weight data are categorized according to 5 truck classifications. A linear regression analysis of the data resulted in a series of equations that will permit evaluation of field-induced stress ranges of a typical girder that occur at midspan, on cover-plate end, and off cover-plate end and are due to standard truck types of known gross weights. These equations were then applied, in conjunction with a damage theory and assumed truck gross weight distributions, to estimate the bridge lives.

•THE PASSAGE of vehicles across highway bridges will induce varying dynamic strains and stresses. Continual application of such loads, if of sufficient magnitude, will cause noticeable permanent distress in the bridge girders and create a limiting bridge fatigue life. It is the purpose of this report to present empirical equations that will permit evaluation of these induced girder stresses. These stresses can then be used, in conjunction with a damage theory, to determine estimated bridge fatigue lives.

The development of the empirical equations is based on extensive field data collected during July and August 1968 by the Civil Engineering Department of the University of Maryland (1, 2). These tests were confined to simply supported, composite girder slab structures, with welded cover plates. The data are limited to the induced stress ranges and corresponding vehicle gross weights.

Although other data such as dynamic variation and mean stress are available and have been tabulated in histogram form, it has been demonstrated (5) that the dominant stress variable for all steels, beam types, and weld details is the stress range. It has also been shown (5) that minimum stress is not significant for cover-plated beams with welded ends. Therefore, the examination and use of the stress-range data in the fatigue analysis of a bridge is relevant.

BRIDGE DESCRIPTIONS

Each bridge in the study was a simply supported composite structure. The locations, characteristics, and properties of a typical interior girder are given in Table 1. Each bridge structure has a tapered cover plate, fillet welded to each girder. The plate width was always less than the girder flange width and had welded ends. Information regarding the spans in each bridge is also given in Table 1; all spans are simply supported.

Bridges 1, 2, and 3 were monitored during a 24-hour period, and bridge 4 was monitored during 7 continuous days. The number of vehicle passages or events used in the data tabulation, which consisted of both strain and vehicle characteristics, are as follows:

Bridge	Events
1	217
2	200
3	92
4	2,565

INSTRUMENTATION AND DATA

Generally, 8 strain gauges were monitored during the field testing of each bridge. The gauges were mounted at 3 possible positions: on and off the cover plate end of the bottom girder flange, bottom flange of girder at longitudinal midspan, and bottom of concrete slab. The particular gauge positions for each bridge tested are given in Table 2. Only the gauge responses at the bottom flange at midspan and at the end of the cover plate will be examined here in detail; the responses of the other gauges are give elsewhere (1, 2).

The basic equipment that was employed to obtain the dynamic records was a Brush light-beam oscillograph and 2 -6 K.C. 4-channel carrier amplifiers. Incorporated into the oscillograph is a time-line generator and a 10-event marker system, which aid in identifying the vehicle records and the vehicle speeds and axle spacings. A telephone was also attached to the event marker and, upon passage of a given vehicle, a given number would be dialed. This signal induced lines on the light-sensitive paper, thus identifying the vehicle that was previously classified on a log sheet.

After passing over the bridge, the truck was directed to a portable weighing station. At the station the distance between axles, the load on each axle, and the identifying number were recorded. After all of the data were collected, the oscillograph paper was edited and then read on the Gerber digital data reduction system. This system translated points on the dynamic records to digital card output. These specified points were selected during the editing of each record.

The loadometer data were also punched on cards so that they could be entered with the corresponding strain data. The tabulation of the strain and loadometer data was then accomplished by a series of computer programs (1, 2). The resulting output for each vehicle passage consisted of record number, body type, axle spacing, gross weight, weight distribution to axles, velocity, number of vibrations, and strain data including maximum dynamic range, maximum dynamic increment, and maximum mean values. These results, in tabular form and card output, were then reprocessed for the development of histograms or regression analyses (4).

An examination of the resulting data (1, 2) indicates that the stress-range response, at various positions on the bridge girder, varies as given in Table 3. These data indicate that the field-induced girder stress ranges due to 70 percent of the truck traffic equal approximately 1.0 ksi.

REGRESSION ANALYSIS

As previously described, the load history data have been reported in detail by Heins and Sartwell (1, 2). Because of the voluminous nature of these data, it was desirable to relate the trends rather than specific data. The field data that were selected were the stress ranges and the corresponding vehicle gross weights and the bridge girder properties.

It was assumed that a linear relationship exists among the following parameters:

$$\sigma_r\,(S/L) = A + B(G) \qquad (1)$$

where

σ_r = induced dynamic stress range on girder, ksi;
G = gross weight of vehicle that induces stress range, kips;
S = elastic section modulus on bottom flange of girder, $in.^3$;
L = girder span length, in.; and
A, B = coefficients obtained from a regression analysis of data.

It should be noted that Eq. 1 will reflect the position of the field strain gauge and corresponding girder property.

The regression analysis represents a linear least square fit of the plotted data, $\sigma_r\,(S/L)$ versus G, along the ordinate and abscissa respectively. The standard deviation or dispersion of the data about this regression line will provide a guide as to the confidence of the data. The standard deviation, $\pm S$, will be measured with reference to the ordinate, $\sigma_r\,S/L$, throughout this study. The linear relationship was selected primarily because of the simplicity of the equation.

The relationships that were developed according to Eq. 1 will have 5 categories for the 3 gauge locations. The 5 categories represent the truck classifications designated as 2D, 3, 2S-1, 2S-2, and 3S-2. These identifications, as shown in Figure 1, generally represent those vehicles that travel through Maryland and can be so classified.

RESULTS

The regression analysis of the modified field data and bridge characteristics resulted in the evaluation of the coefficients A and B for each truck type and gauge location, as given in Table 4. The data that were used to establish these constants comprised the composite data collected during the monitoring of all 4 bridge structures. The modulus of elasticity of steel was assumed equal to 29×10^3 ksi.

Plots of the regression lines for the 5 truck classifications and girder positions are given in Figures 2, 3, and 4. Figure 2 shows the regression line of the data observed on the cover plate end; Figure 3, the plot of data observed off the cover plate end; and Figure 4, the trends at the midspan of the girder.

The standard deviations about the regression equations are also given in Table 4. Generally, the dispersions about the mean line, for 95 percent of the population, is ±0.20 kip.

Figure 3 shows that the curves for truck types 2D and 3 and those for types 2S-1, 2S-2, and 3S-2 can be combined into 2 curves as shown in Figure 5. These combinations will yield the following general equations:

$$\sigma_r\ (S/L) = 0.0715 + 0.0245\ (G) \tag{2}$$

for truck types 2D and 3, and

$$\sigma_r\ (S/L) = 0.1211 + 0.0153\ (G) \tag{3}$$

for truck types 2S-1, 2S-2, and 3S-2.

These equations are important for cover-plated beams, for they represent the response of the beam at that location that governs the fatigue life (3, 5). These equations are only applicable for those bridges examined in this study.

BRIDGE LIFE

Damage Theories

The usefulness of the equations just described can be demonstrated by examining the probable fatigue life of a given bridge. The probable fatigue life of a given bridge may be referenced to the behavior of a single member of that system. Because the vehicles and thus loads that cross the structure are random, some cumulative damage criteria should be applied. The most common damage criterion that is currently being applied is Miner's hypothesis (7).

The evaluation of stress ranges for the many vehicles crossing a bridge would be a tremendous task. However, by the application of Eqs. 2 and 3 and the use of the gross-weight data for the various vehicles crossing a given bridge, the induced stress ranges can be readily computed.

The damage criterion is expressed as

$$\sum (n/N_f) = 1 \tag{4}$$

where n and N_f are as defined previously (7).

Estimated Bridge Life

The linear damage criterion will now be applied in estimating the fatigue life of the 4 bridges under study. To apply Miner's equation (4) requires the number of load applications, n, at a given stress range and the corresponding failure life. The traffic pattern, thus vehicle classifications and weights, for the respective 4 bridges must be determined. A statistical technique and computer program have been developed (5)

Table 1. Location and characteristics of test bridges.

Characteristic	Bridge 1	Bridge 2	Bridge 3	Bridge 4
Location	I-83S over Bunker Hill Road near Hereford	US-301 over MD-5 near Waldorf	US-1 over I-495	US-301 over Western Branch Creek
Slab thickness, in.	7	7	7	7
Girder				
Number	8	8	7	7
Spacing	5 ft 11 in.	5 ft 3 in.	7 ft 2 in.	7 ft
Span				
Number	3	2	5	3
Length	27 ft 7 in., 47 ft[a], 22 ft	76 ft	38[a], 42, 77, 84, 36 ft	42[a], 52, 42 ft
Roadway width, ft	39	30	39	40
Size	27WF76	36WF194	27WF84	27WF97
Cover plate	12 in. × 11/16 in. × 33 ft	10 in. × 7/8 in. × 43 ft	7 in. × 1/2 in. × 24 ft	6 in. × 5/8 in. × 25 ft
Section modulus, s, at bottom, in.^{3}				
With cover plate	471.5	1,158.0	411.0	464.0
Without cover plate	264.0	835.0	318.0	358.0
s/L, in.				
With cover plate	0.835	1.260	0.986	0.920
Without cover plate	0.468	0.908	0.765	0.710

[a]Test span length.

Table 2. Gauge locations on bridges.

Bridge	Number of Gauges	Location
1[a]	2	Off end cover plate at one end of girder 4
	2	On end cover plate at one end of girder 4
	2	Off end cover plate at one end of girder 5
	2	On end cover plate at one end of girder 5
2[a]	1	Off end cover plate at one end of girder 5
	1	On end cover plate at one end of girder 5
	1	Off end cover plate at one end of girder 6
	1	On end cover plate at one end of girder 6
	1	Midspan of girder 3
	1	Midspan of girder 4
	1	Midspan of girder 5
	1	Midspan of girder 6
3	3	Midspan
	5	Bottom of slab
4[b]	2	Off end cover plate at each end of girder 4
	2	On end cover plate at each end of girder 4
	1	Midspan of girder 3
	1	Midspan of girder 4
	1	Midspan of girder 5
	1	Midspan of girder 6

[a]8-girder system. [b]7-girder system.

Figure 1. Truck classifications.

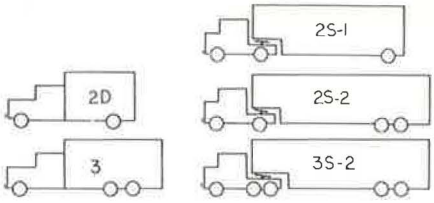

Table 3. Stress-range responses at various gauge locations.

Bridge	Gauge Location	Variation (ksi)	70 Percent (ksi)	1 Percent (ksi)
1	Off cover plate	0.1 to 2.0	0.7	1.8
	On cover plate	0.1 to 0.9	0.3	0.7
2	Midspan	0.1 to 6.0	0.8	6.0
3	Off cover plate	0.2 to 2.6	0.8	2.5
	On cover plate	0.1 to 1.6	0.6	1.5
	Midspan	0.2 to 2.6	0.8	2.5
4	Off cover plate	0.1 to 4.3	1.0	3.0
	On cover plate	0.1 to 3.6	0.5	2.0
	Midspan	0.1 to 5.6	1.2	3.4

Table 4. Equation coefficients and standard deviations.

	On Cover Plate			Off Cover Plate			Midspan		
Truck Type	Coefficient A	Coefficient B	Standard Deviation (kip)	Coefficient A	Coefficient B	Standard Deviation (kip)	Coefficient A	Coefficient B	Standard Deviation (kip)
2D	0.0625	0.0198	0.115	0.0254	0.0257	0.055	0.1122	0.0330	0.080
3	0.1205	0.0175	0.140	0.0840	0.0236	0.080	0.2547	0.0326	0.106
2S-1	0.1808	0.0105	0.130	0.1464	0.0136	0.070	0.2746	0.0178	0.101
2S-2	0.0840	0.0125	0.180	0.0699	0.0150	0.100	0.1740	0.0227	0.123
3S-2	0.1740	0.0110	0.210	0.1341	0.0139	0.107	0.5530	0.0147	0.121

Figure 2. Stress range on cover plate, Eq. 1.

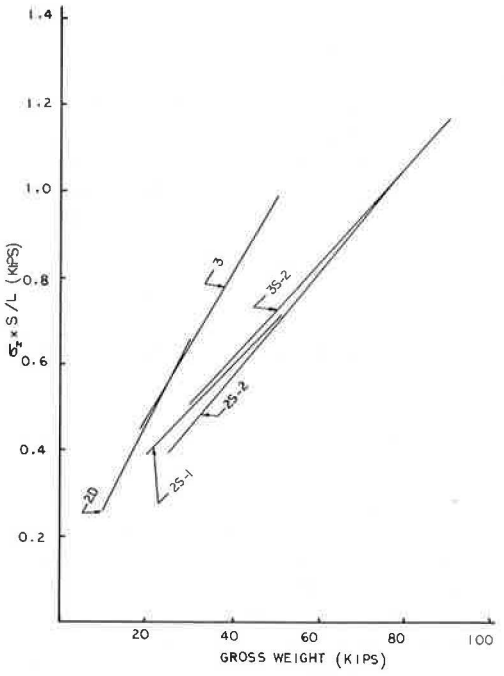

Figure 3. Stress range off cover plate, Eq. 1.

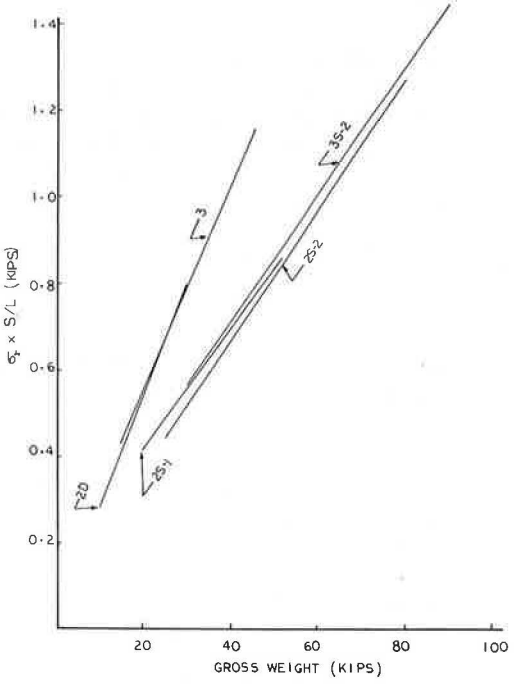

Figure 4. Stress range at midspan, Eq. 1.

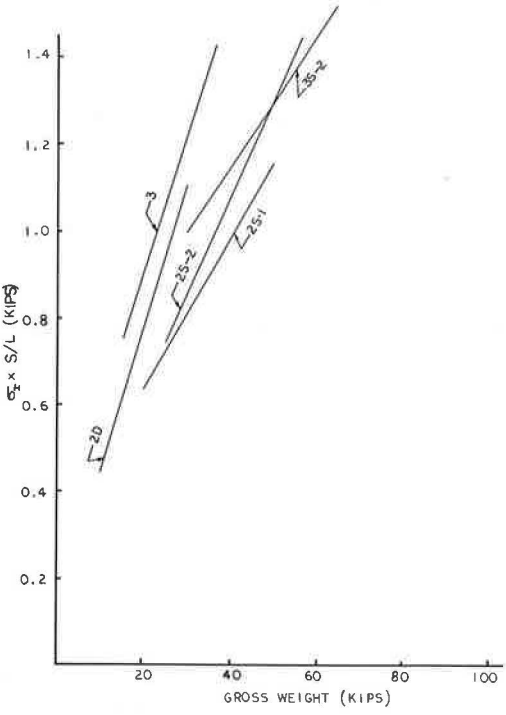

Figure 5. Stress range off cover plate, Eqs. 2 and 3.

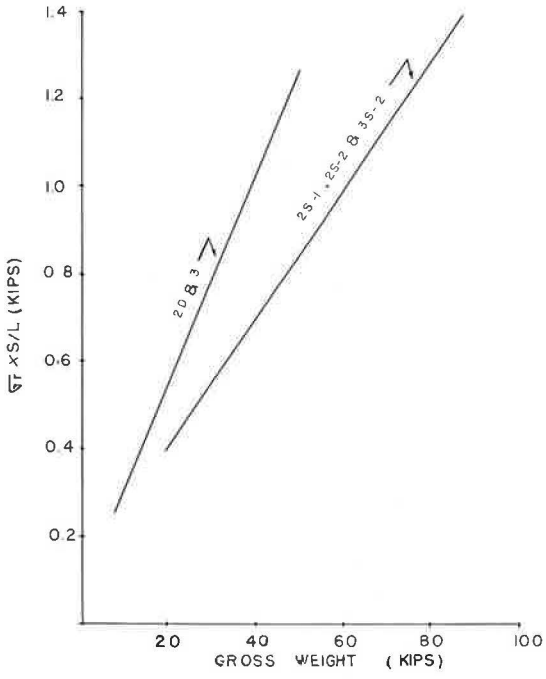

Table 5. Estimated fatigue life.

Bridge	Annual Damage	Existing Service Life (year)	Estimated Fatigue Life (year)
1	0.000006175	21	162,000
2	0.007900	20	127
3	0.00006025	7	16,650
4	0.001064	12	940

that will predict the frequency of types and gross weights of vehicles for an average day at a given sector in Maryland. This technique utilizes the loadometer data collected throughout the state by the state transportation department. Applying the computer program (5) yielded the traffic data for the respective bridges.

Based on the assumption that the frequency of loads for a typical day was the same throughout the year, the estimated damage for a year was determined and is given in Table 5. If the damage or vehicle loadings do not vary from year to year, the fatigue life of the bridge can be estimated by the following equation:

$$N \text{ life} = 1 / \sum (n/N_t) \quad (5)$$

Certainly, the great variation in predicted life indicates a need for better truck volume data and continued fatigue studies.

SUMMARY AND CONCLUSIONS

Examination of field data, induced girder strains, and corresponding vehicle type and gross weight from 4 simply supported girder slab bridges has yielded a series of empirical equations relating induced stresses and vehicle gross weights. These equations were then employed in conjunction with a linear damage theory and estimated vehicle weight and volume data to predict the fatigue life of the 4 bridge structures. A wide variation in fatigue life of those bridges resulted from this analysis.

The methodology for using the collected load history data to develop equations that can be used in fatigue analysis and eventually design is promising. Additional data are certainly required in order to provide some degree of confidence in the empirical equations. Possibly an integrated analysis of all loading history data now being collected nationwide (9) should be considered.

ACKNOWLEDGMENTS

The collection and reduction of data and the fatigue analysis are part of a project at the University of Maryland sponsored by the Maryland Department of Transportation and the Federal Highway Administration. Appreciation is expressed for their support and guidance during this research.

REFERENCES

1. Heins, C. P., and Sartwell, A. D. Tabulation of 24-Hour Dynamic Strain Data on Four Simple Span Girder-Slab Bridge Structures. Univ. of Maryland, College Park, Civil Eng. Rept. 29, June 1969.
2. Sartwell, A. D., and Heins, C. P. Tabulation of Dynamic Strain Data on a Girder-Slab Bridge Structure During Seven Continuous Days. Univ. of Maryland, College Park, Civil Eng. Rept. 31, Sept. 1969.
3. Murad, F. A., and Heins, C. P. Fatigue of Beams With Welded Cover Plates. Univ. of Maryland, College Park, Civil Eng. Rept. 38, Sept. 1970.
4. Khosa, R. L., and Heins, C. P. Study of Truck Weights and the Corresponding Induced Bridge Girder Stresses. Univ. of Maryland, College Park, Civil Eng. Rept. 40, Feb. 1971.
5. Fisher, J. W., et al. Effects of Weldments on the Fatigue Strength of Steel Beams. Lehigh Univ., Bethlehem, Penn., Rept. 334.2, Sept. 1969.
6. Galambos, C. F., and Heins, C. P. Loading History of Highway Bridges, Comparison of Stress Range Histograms. Highway Research Record 354, 1971, pp. 1-12.
7. Miner, M. A. Cumulative Damage in Fatigue. Jour. of Applied Mechanics, June 1945.
8. Desrosiers, R. D. The Development of a Technique for Determining the Magnitude and Frequency of Truck Loadings on Bridges. Univ. of Maryland, College Park, Civil Eng. Rept. 24, April 1969.
9. Galambos, C. F., and Armstrong, W. L. Acquisition of Loading History Data on Highway Bridges. Public Roads, Vol. 35, No. 8, June 1969.

LOADING HISTORY STUDY OF TWO HIGHWAY BRIDGES IN VIRGINIA

Wallace T. McKeel, Jr., Charles E. Maddox, Jr., and Henry L. Kinnier,
Virginia Highway Research Council; and
Charles F. Galambos, Federal Highway Administration

An evaluation was made of the stress ranges in 2 typical highway bridge spans, a 76-ft steel beam composite span and a 60-ft prestressed concrete beam span, under service loadings. The strains at selected points on the superstructure elements of the spans were recorded continuously for periods of 4 and 5 days under normal traffic conditions by an automatic computer controlled data acquisition system and converted to stress on the basis of assumed moduli of elasticity. The weights, axle spacings, and lateral positions of trucks crossing the instrumented spans during the test periods were also recorded. The magnitudes of all stress ranges measured in the 2 simply supported test spans were low, and it was concluded that both structures were safe from fatigue distress under current load limitations. Stress ranges of a magnitude comparable to that in the main supporting elements were recorded in the midspan diaphragm of the steel beam span, and higher stress ranges were recorded in the deck reinforcement.

•MANY field tests of bridges, employing loading by a variety of test vehicles, have been conducted during the past several years; but there have been very few studies of the stresses produced by normal truck traffic, largely because of difficulties involved in obtaining the data with existing strain-measuring equipment. An instrumentation system that provides a practical means of assessing the structural behavior of bridges under service loadings was developed under a contract awarded by the Federal Highway Administration (1). After delivery of the system in 1966, FHWA inaugurated a nationwide program of cooperative studies guided by committees of the American Society of Civil Engineers and the Highway Research Board. One such study, reported here, was begun in Virginia in July 1968.

The primary purpose of the Virginia study was to experimentally determine and evaluate the stresses produced by service loadings at selected points on the superstructures of 2 typical, modern highway bridges in Virginia. One span on each bridge was instrumented, and data were collected continuously during periods of 4 to 5 consecutive days at each structure. A theoretical analysis verified the magnitude of the strains measured during the experimental phase of the study.

EXPERIMENTAL PROCEDURE

The 2 structures included in the study, a steel beam composite span bridge carrying the northbound lane of Interstate 95 over Quantico Creek and Va-629 near Dumfries and a prestressed concrete beam bridge carrying the northbound lane of Interstate 81 over Cedar Creek near Middletown, were chosen because of their proximity to permanent weighing stations that were in operation 24 hours a day. In general, the experimental procedure included monitoring strains at selected points on the superstructures and noting the type and lane position of all trucks crossing the bridge. Separate records of axle weights and spacings were kept at the nearby weighing stations for correlation

with the vehicle data taken at the bridge. The trucks were classified by the axle types shown in Figure 1 in conjunction with a body description, such as van, flatbed, tank, or car carrier, and an identification of the operating company. The traffic volumes were such that weighing station records were completed on slightly more than 85 percent of the trucks crossing the test structures.

The automated, computer-controlled data acquisition system developed for the FHWA has been described in detail in other publications (1, 2), and only a summary of its functions will be given here. Essentially, the equipment, which was housed in a trailer under the bridge, took the output from a maximum of 10 resistance strain gauges in the form of analog voltages, digitized the voltages, and stored and tabulated strain ranges for printing out at specified intervals.

The printed output consisted of the number of occurrences of strain ranges at each of 9 preselected levels for each of 10 gauges on the structures. The computer was programmed to ignore strain ranges below a minimum test level in order to eliminate the effect of automobiles crossing the span. A strain range was measured from peak to valley; the computer sought a peak strain when the signal exceeded the minimum test level, and it sought a valley when the signal dropped to or below the zero level. An event was counted each time the signal passed the minimum test level and returned to zero. It was not uncommon for a single truck to produce more than one strain range above the minimum test level.

I-95 BRIDGE TEST

The bridge carrying the northbound lane of I-95, located in a generally urban environment 30 miles south of Washington, contains a series of 3 simply supported steel beam composite spans 69 ft in length and 1 span 76 ft in length. Average daily traffic volumes at the site during the years 1968 to 1970 are given in Table 1, which also gives the percentage of trucks and buses (3). The buses, which were not required to stop at the weighing station, constitute only 1 percent of the traffic.

The instrumented span, shown in Figure 2, measures 74 ft 6 in. center-to-center of the bearings (1). The supporting elements are six 36-in. wide flange beams with partial length cover plates over the central portion of the span. Welded stud shear connectors ensure composite action between the beams and the 8-in. concrete deck. For the purposes of this study the beams were numbered 1 through 6 from the east side of the structure, as shown in Figure 2. The 42-ft clear roadway is divided into 3 traffic lanes, numbered from the east side of the bridge such that lane 1 is the right lane.

Gauge positions are referred to by number; gauges 1 to 5 were at the midspan of beams 1 to 5, centered on the bottom surface of the lower flange cover plate, and gauges 6 to 8 were approximately 4 in. beyond the ends of the cover plates on beams 1, 2, and 3. Gauge 9 was placed on a transverse (main) reinforcing bar in the lower level of the deck steel, near the point of maximum positive moment in the slab. Gauge 10 was placed on the bottom flange of the midspan diaphragm, midway between beams 2 and 3.

Traffic Data

The test ran continously at the I-95 site for a period of 105 hours, during which time there were 98 sampling periods of 1 hour's duration each. The remaining time was consumed by the printing of the data; strains were not monitored during the printing operation. Approximately 6,906 trucks crossed the bridge during the sampling periods, and records were obtained at the weighing station for 5,916 of those vehicles, approximately 85 percent of those reported at the structure.

The percentage of trucks in each of 8 weight ranges are shown in Figure 3 for each of the 3 traffic lanes and for the bridge as a whole. More than three-fourths of the trucks crossed the structure in the right traffic lane, and less than 1 percent used the passing lane.

Some overloaded vehicles may have left the highway at an interchange between the bridge and the weighing station, but statistics supplied by the Virginia Department of

Figure 1. Axle type designations.

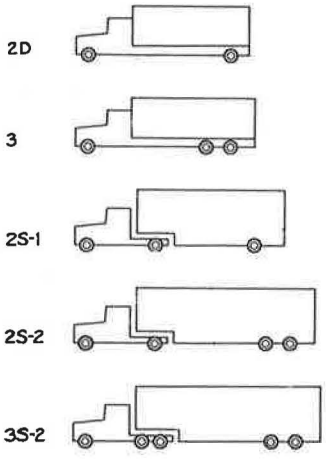

Table 1. Average daily traffic volumes on I-95 bridge.

Year	All Vehicles	Trucks				Buses
		Type 2D	Type 3	Types 2S-1, 2S-2, and 3S-2	Total	
Number						
1968	15,060	620	30	2,000	2,650	160
1969	16,160	1,000	35	2,100	3,135	175
1970	18,185	1,120	65	2,150	3,335	150
Percent						
1968	100	4.1	0.2	13.3	17.6	1.1
1969	100	6.2	0.2	13.0	19.4	1.1
1970	100	6.2	0.3	11.8	18.3	0.8

Figure 2. Details of instrumented span on I-95 bridge.

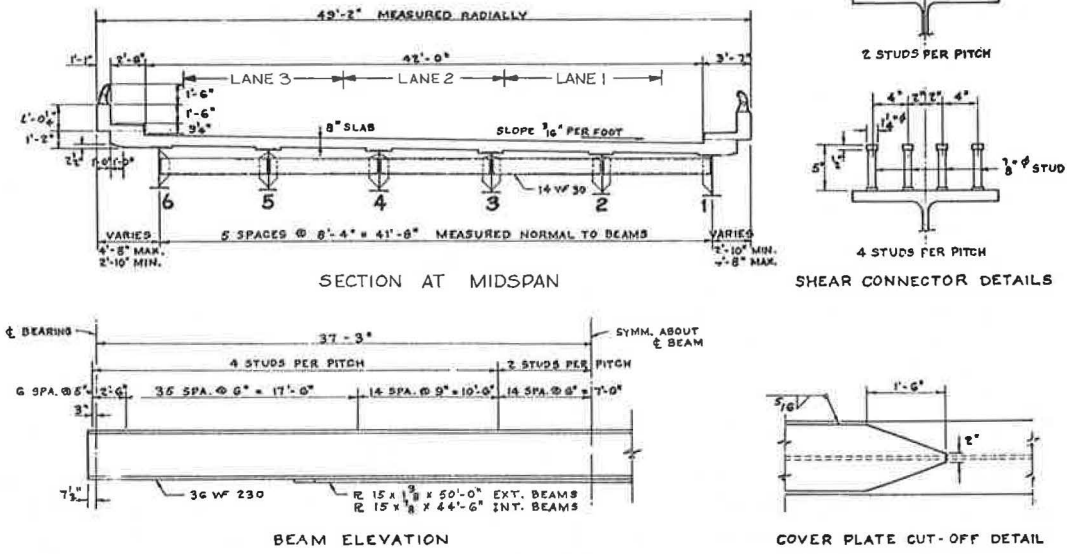

Figure 3. Percentage of trucks by weight range on I-95 bridge.

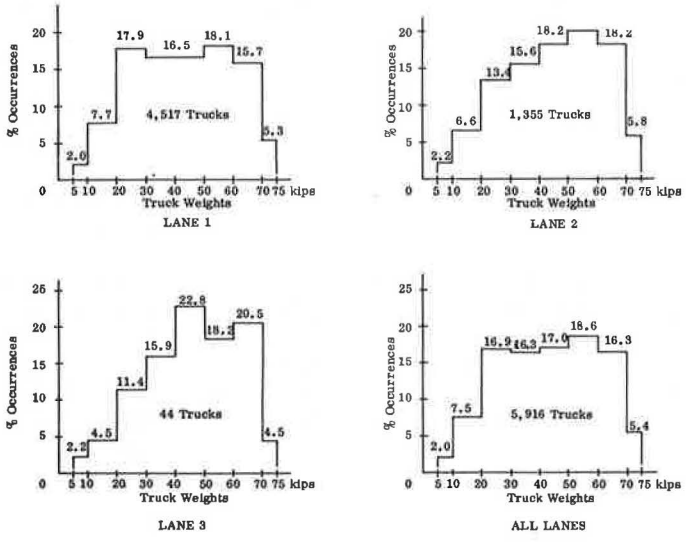

Highways indicate that only a few severely overloaded vehicles would be expected. The weight limitations in Virginia are effectively enforced through the use of both permanent weighing stations and mobile units, and only 0.5 percent or fewer of the vehicles weighed by all units since 1956 have been overweight (4).

The Virginia Code limits the single axle weight of any vehicle or combination to no more than 18,000 lb and the tandem axle weight to no more than 32,000 lb. The gross weight is limited by the distance between the extremes of all axles under the vehicle or combination, and the maximum gross weight is 70,000 lb for a vehicle having a length of 42 ft between the extremes of its axles (5). Conventionally, though not by law, a 5 percent tolerance is allowed. The weighing station data obtained during the study reflect the requirements of the code; no vehicles heavier than 75,000 lb in gross weight were recorded.

Stress Data

The primary purpose of this experimental study was to determine the stress ranges produced by service loadings at selected points on the instrumented span. The strain ranges given in the printouts from the data acquisition system were combined and tabulated for each of the 10 gauges and converted to stress; the modulus of elasticity of steel was assumed to be 30×10^6 psi. The combined data are given in Table 2 for each gauge except gauge 6, which behaved erratically throughout the tests. The minimum test level was set at a strain of 15 μ in./in. (450-psi stress) for gauges 1 to 7 and 40 μ in./in. (1,200 psi) for gauges 8 to 10.

Figure 4 shows the percentage of occurrence of events in each strain range for the midspan gauges on the bottom of the lower flanges of beams 1 to 5. The histograms exhibit shape characteristics similar to those reported previously by other researchers (1, 2). The strain ranges recorded in the beams were quite low, but there is no reason to doubt their accuracy. The experimental results are similar to those obtained in an earlier study conducted at the same bridge by the FHWA (1).

The highest stress ranges recorded at a midspan gauge were in beam 4 (gauge 4), which experienced 2 occurrences of ranges between 3,150 and 3,600 psi. A single occurrence of a range between 3,600 and 4,200 psi was recorded at gauge 8, which was located 4 in. beyond the end of the lower flange cover plate on beam 3. The greatest number of stress ranges between 1,350 and 2,700 psi occurred in beams 2 and 3, and beam 1 experienced the greatest number of low stress ranges.

Beams 2 and 3 had the greatest number of relatively high stress ranges because, as indicated by the typical section shown in Figure 2, they are the supporting elements beneath the right lane, in which more than three-fourths of the trucks crossed the structure. Beam 1 is under the curb at the edge of the roadway. Beams 3 and 4 are the supporting elements for the center lane, which carries fewer trucks, and beams 5 and 6 are under the seldom used left lane. Although beams 4 and 5 experienced more stress ranges above 2,700 psi, the much greater number of loadings between 1,350 and 2,700 psi in beams 2 and 3 would have more influence on the service life of the structure.

Fortunately, the service life of the beams is not critical. Most of the stress ranges to which the girders were subjected under loading by the approximately 6,906 trucks crossing the structure during the tests were below 2,250 psi. Very few stress ranges greater than approximately 3,000 psi were recorded, and it was concluded that the girders can safely accommodate an increased volume of truck traffic under the current weight limitations. An increase in the allowable weight limits was not recommended for reasons that will be discussed later in the paper.

Several occurrences of stress ranges above 3,000 psi were recorded at gauge 10 on the lower flange of the diaphragm between beams 2 and 3. Relatively little is known about the loadings to which diaphragms are subjected, but it is apparent that the stress in these members is comparable to, and in some instances greater than, the measured stress in the girders. It should be realized, however, that the stresses in both the girders and the diaphragm were low in comparison to allowable design stresses. The highest stress ranges encountered in this study occurred in the transverse deck re-

Table 2. Occurrences in each strain range at gauges on I-95 bridge.

	15 μin./in. Minimum								40 μin./in. Minimum				
Strain Level	Strain Range (μin./in.)	Stress Range (psi)	Gauge 1	Gauge 2	Gauge 3	Gauge 4	Gauge 5	Gauge 7	Strain Range (μin./in.)	Stress Range (psi)	Gauge 8	Gauge 9	Gauge 10
0			0	0	0	0	0	0			0	4	0
1	135	4,050	0	0	0	0	0	0	200	6,000	0	3	0
2	120	3,600	0	0	0	2	0	0	180	5,400	0	13	1
3	105	3,150	0	2	7	10	8	2	160	4,800	0	61	2
4	90	2,700	1	81	82	39	15	42	140	4,200	1	316	10
5	75	2,250	58	809	548	227	31	642	120	3,600	7	718	90
6	60	1,800	905	1,985	2,054	714	106	1,993	100	3,000	55	1,169	803
7	45	1,350	4,646	3,669	3,914	3,167	1,073	3,874	80	2,400	703	1,422	1,186
8	30	900	4,481	2,935	2,680	4,539	2,738	3,602	60	1,800	2,050	1,133	2,026
9	15	450							40	1,200			
Total			10,084	9,481	9,285	8,698	3,971	10,155			2,816	4,839	4,118

Note: Data for gauge 6 were discarded because of erratic behavior.

Figure 4. Occurrences in each strain range at gauges 1 to 5 on I-95 bridge.

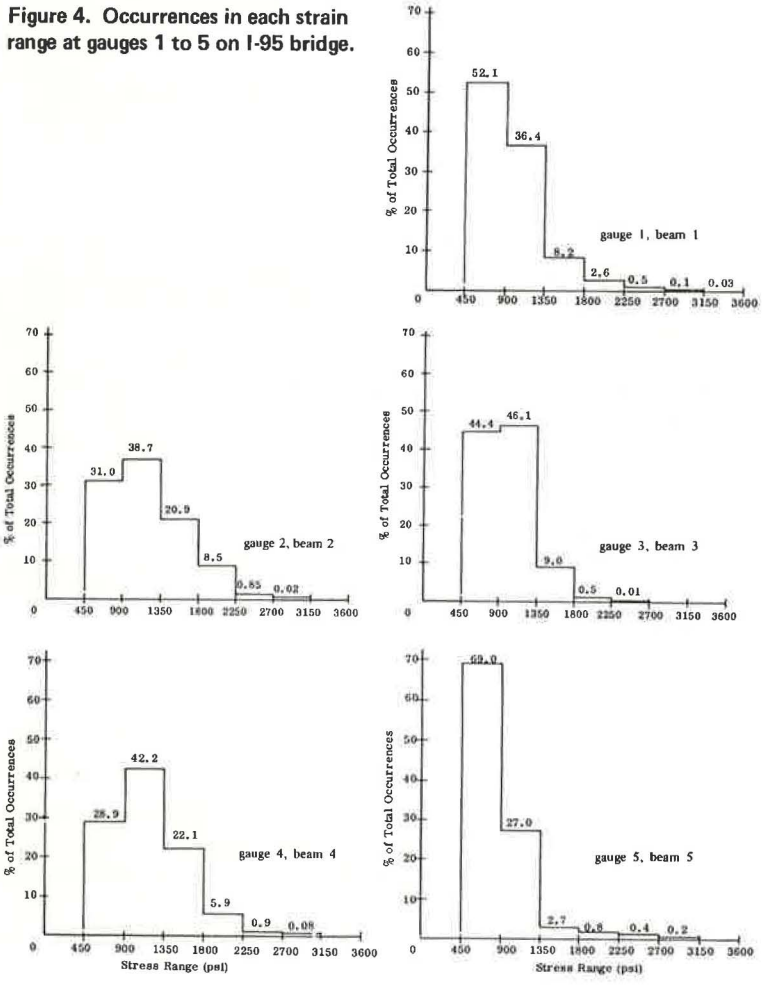

inforcing bar (gauge 9). The combination of the magnitude of the stress ranges and the number of repetitions recorded is not considered critical.

It was not unusual for a single truck to produce more than one strain range above the minimum test level. The total number of strain range events given in Table 2 indicates that the 6,906 trucks crossing the structure caused an average of approximately 1.3 strain events above 450 psi per vehicle in beams 2 and 3 and nearly 1.5 per vehicle in beam 1. This finding is of more interest than importance because both the minimum test level and the recorded strain ranges were low. The data acquisition system utilized in the tests did not allow a determination of the magnitudes of the subsequent strain ranges, but research of this nature is planned by the FHWA.

I-81 BRIDGE TEST

The second structure tested, the bridge carrying the northbound lane of I-81 over Cedar Creek, presents contrasts to the I-95 bridge in both design type and traffic volume. The I-81 bridge, which is typical of many prestressed concrete bridges throughout Virginia, is composed of five 60-ft prestressed concrete beam spans, one of which was instrumented, and one 85-ft prestressed concrete beam span. The average daily traffic volume and the percentage of trucks and buses for the years 1968-1970, are given in Table 3 (3). The traffic volume at this relatively rural site is much less than that at the I-95 test location.

The instrumented span on the I-81 bridge was a prestressed concrete beam span, 58 ft 3 in. in length, center-to-center of the bearings. Figure 5 shows that the 8-in. thick concrete deck is supported on 5 AASHO type 3 prestressed beams. The beams are numbered 1 to 5 from the right side of the bridge facing the direction of traffic flow. Cast-in-place concrete diaphragms are located on the skew angle at midspan and over the bearings. The 30-ft clear roadway is divided into 2 traffic lanes, which are numbered from the right as before. Ten type A-93 concrete strain gauges were mounted on the surfaces of the concrete beams at midspan, in the positions shown in Figure 5.

Traffic Data

The I-81 test ran continuously for a period of 84 hours, but approximately 12 hours of sampling were lost because of equipment malfunction. Approximately 2,616 trucks crossed the bridge during 69 sampling periods, and weighing station records were completed on 2,276, or 87 percent of the vehicles.

Figure 6 shows the percentage of the trucks in each of 8 weight ranges for both traffic lanes and the bridge as a whole. As in the case of the I-95 bridge, most of the trucks, almost 98 percent at this site, crossed the structure in the right lane. The I-81 traffic differs from that on I-95 in that the population distribution is skewed toward a higher percentage of heavy trucks.

Stress Data

The number of occurrences at each strain range are given in Table 4. The stresses shown are based on the use of a modulus of elasticity of 4.34×10^6 psi for the prestressed concrete, obtained through the ACI formula (6)

$$E = W^{1.5} (33) f_c'$$

where W is the weight of the concrete per cubic foot, assumed to be 150 lb, and f_c' is the compressive strength of the concrete, assumed to be 5,000 psi. The minimum test level was set at 10.1 μ in./in. of strain, or 43.8 psi.

The data given in Table 4 indicate that beam 2, which is located directly beneath the right lane, is subject to the greatest number of occurrences of the higher stress ranges, those above 130 psi. Likewise beams 4 and 5 under the left lane, which is seldom used by trucks, have significantly fewer occurrences of ranges above 130 psi. This sensitivity to the path of the vehicles was also evident on the case I-95 bridge. Beams 1 and

Table 3. Average daily traffic volumes on I-81 bridge.

Year	All Vehicles	Trucks				Buses
		Type 2D	Type 3	Types 2S-1, 2S-2, and 3S-2	Total	
Number						
1968	3,255	335	12	700	1,047	8
1969	3,422	355	8	750	1,113	10
1970	3,692	400	75	750	1,225	18
Percent						
1968	100	10.3	0.4	21.5	32.2	0.2
1969	100	10.4	0.2	21.9	32.5	0.3
1970	100	10.8	2.0	20.3	33.1	0.5

Figure 5. Details of instrumented span on I-81 bridge.

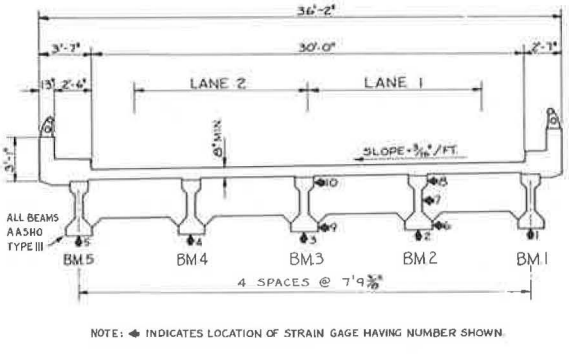

Figure 6. Percentage of trucks by weight range on I-81 bridge.

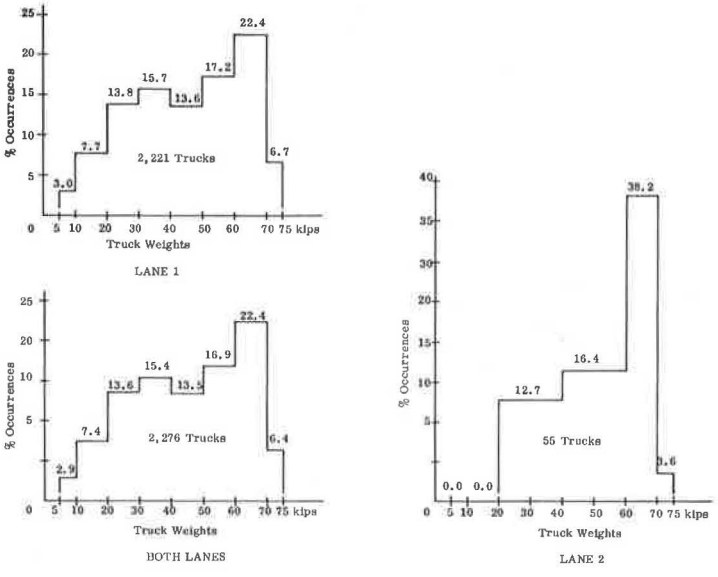

3 were more equitably loaded on the I-81 bridge than on the I-95 structure, possibly because the stiff cast-in-place concrete diaphragms distributed the load.

Gauges 6-10 located on the side surfaces of beams 2 and 3 show the expected decrease in stress as the gauge position approaches the location of the neutral axis. The data for those gauges also tend to verify the values obtained at the midspan lower flange gauges.

The data indicate that most of the strain ranges recorded at any of the instrumented points on the surfaces of the girders were below 130 psi, and the highest ranges, 3 occurrences recorded in beams 1 and 2, were below 300 psi. The stress ranges in the embedded steel can be assumed to be higher by a factor equal to the modular ratio, but they are also of a low order of magnitude. Fatigue is, therefore, unlikely to present any problems on this bridge under currently allowable service loads.

THEORETICAL ANALYSIS

A theoretical analysis was performed to verify the magnitudes of the low stress ranges recorded in the experimental phase of the study. The experimentally determined stress ranges were, of course, much lower than the design stresses computed in accordance with the AASHO specifications. In the analysis, the extreme fiber stresses at midspan of the girders resulting from the individual truck loadings, as recorded at the weighing station, were computed and compared to the midspan stress ranges obtained in the field. The comparison was made for ten 1-hour data sampling periods at the I-95 bridge and 4 hours on the I-81 bridge. The hours selected for comparison were those in which the truck weight records were complete. A brief description of the analytical methodology is given in the following paragraphs.

Beam theory was used to develop an algorithm for the magnitude of the maximum moment at midspan, which occurs in a simple span when the middle axle of a 3-axle truck is over the center of the span. Only one strain event per vehicle was assumed, and the effect of impact due to dynamic loading was not considered. The individual truck data obtained at the weighing station plus the lane in which the vehicle crossed the structure composed the loading input. The maximum moments caused by all trucks were distributed to the beams on the basis of factors computed for a representative vehicle, a 3-axle truck with axle spacings of 10 and 30 ft and weights of 10 kips on the front axle and 30 kips on the middle and rear axles, at the position of maximum moment in the right and center lanes. The very few trucks in the left lane were ignored.

Classical finite difference theory was used to determine the distribution factors. The deflection of the deck under any loading condition was expressed in terms of a symmetrical grid composed of 7 points equally spaced along each of the 6 beams of the I-95 bridge and the 5 beams of the I-81 bridge.

The basis for the distribution factor analysis was an evaluation of the transverse and longitudinal stiffnesses, assuming no torsional restraint, at each of the grid points. This assumption of pinned intersection points may be inaccurate in the case of a heavily skewed bridge, but it was considered acceptable in the case of the 2 test spans, which were skewed at 3 deg 46 min on the I-95 bridge and 13 deg 33 min on the I-81 bridge. Evaluation of the transverse stiffnesses revealed that the W14 x 30 diaphragms on the steel beam bridge could be ignored, but the stiffnesses of the heavy cast-in-place concrete diaphragms on the prestressed beam bridge had to be included. The beams were assumed to be hinged at the points of intersection to allow both rotational and translational independence except for continuity of vertical deflection. The conditions of compatibility were identical to those of a stiffened plate.

The theoretical analysis was successful in verifying the general magnitudes of the experimentally determined stress ranges. However, the correlation between the number of stress range events predicted by theory and the number measured in the field was less than perfect. The theoretical analysis consistently predicted fewer stress events above the minimum test level than were actually recorded at the I-95 site; that indicated the need for refinements to account for impact and the effect of a single vehicle in producing more than one recorded stress range. These factors are difficult to include in the analysis. The impact factor varies widely with the roughness

Table 4. Occurrences in each strain range at gauges on I-81 bridge.

Level	Strain Range (μin./in.)	Stress Range (psi)	10.1 μin./in. Minimum									
			Gauge 1	Gauge 2	Gauge 3	Gauge 4	Gauge 5	Gauge 6	Gauge 7	Gauge 8	Gauge 9	Gauge 10
0			0	0	0	0	0	0	0	0	0	0
1	90.9	394.2	0	0	0	0	0	0	0	0	0	0
2	80.8	350.4	0	0	0	0	0	0	0	0	0	0
3	70.7	306.6	2	1	0	0	0	0	0	0	0	0
4	60.6	262.8	2	7	3	1	0	2	0	0	0	0
5	50.5	219.0	2	18	7	0	0	8	1	0	2	0
6	40.4	175.2	68	226	84	29	2	145	2	1	28	16
7	30.3	131.4	887	950	1,069	91	16	1,120	6	5	789	53
8	20.2	87.6	1,963	992	1,237	1,013	233	1,365	213	31	1,433	69
9	10.1	43.8										
Total			2,924	2,194	2,400	1,134	251	2,640	222	37	2,252	138

Table 5. Average weights and axle spacings of trucks on I-95 and I-81 bridges.

Truck Type	I-95 Bridge			I-81 Bridge								
							Axle Weight (kip)			Axle Spacing (ft)		
	Number	Percent	Gross Weight (kip)	Number	Percent	Gross Weight (kip)	Front	Middle	Rear	Front-Middle	Middle-Rear	Overall
2D	542	9.3	14.63	272	10.9					14.0	—	14.0
3	82	1.4	27.54	26	1.0	22.35	7.16	15.19	—	14.0	—	14.0
2S-1	432	7.4	27.92	139	5.6	29.67	7.15	11.54	10.98	11.0	29.0	40.0
2S-2	1,725	29.7	41.14	473	18.9	38.51	8.07	13.20	17.25	11.0	27.0	39.0
3S-1	7	0.1	35.76	2	0.1	37.20	6.55	22.70	7.95	14.0	20.0	34.0
3S-2	3,029	52.1	53.37	1,591	63.6	54.86	8.66	23.40	22.80	12.0	30.0	42.0
All	5,817	100.0	43.86	2,503	100.0	45.48	8.01	19.10	18.37	12.0	26.0	38.0

Table 6. Standard deviations of average weights and axle spacings of trucks on I-95 and I-81 bridges.

Truck Type	I-95 Bridge	I-81 Bridge						
			Axle Weight			Axle Spacing		
	Gross Weight	Gross Weight	Front	Middle	Rear	Front-Middle	Middle-Rear	Overall
2D	5.44	5.51	2.23	3.90	—	4.46	—	4.46
3	12.32	9.99	2.27	8.25	—	3.05	—	3.05
2S-1	7.69	15.93	1.33	7.39	8.30	1.30	7.23	8.47
2S-2	10.55	9.86	1.25	3.50	6.23	3.64	7.04	5.55
3S-2	11.60	0.28	0.21	0.71	0.78	1.41	7.07	8.49
3S-2	14.90	13.96	1.00	6.69	7.46	2.83	4.67	7.36
All	17.59	18.95	1.77	8.38	10.12	3.24	10.34	11.15

of the approach surface, the vehicle suspension characteristics, and the states of oscillation of the vehicle and the span. The number of recorded stress ranges per vehicle crossing the spans can be expected to vary among structures, as it did in this study. A maximum of 1.1 strain events per crossing vehicle was recorded at the I-81 site, and 1.3 to 1.5 events per vehicle were recorded at the I-95 site.

The agreement between the theoretical and experimental numbers of stress events was better for the I-81 prestressed beam span, possibly because of the lower number of strain events per corssing vehicle. However, for the concrete structure, the analysis consistently predicted more events above the minimum test level than were recorded in the field. This error may be due, in part, to the selection of an inaccurate modulus of elasticity of the concrete.

Space limitations do not allow the inclusion in this paper of the several diagrams that fully illustrate the correlation attained through the application of the theoretical analysis to the test structures. These are shown in the final report for the study.

STATISTICAL CHARACTERISTICS OF TRUCK POPULATIONS

The weighing station data obtained in both the I-95 and the I-81 bridge tests were analyzed statistically to determine average axle and gross weights and average axle spacings. Only the gross weight data from the I-95 test were considered valid because of an inconsistency in recording the data for the individual axles, but the average axle weights and spacings obtained during the I-81 test are considered representative of both populations. The magnitudes of the truck populations are slightly larger than those shown previously because all trucks, including those that crossed the structure while the strain monitoring equipment was inactive, are considered.

The average axle weights and spacings obtained for each truck type are given in Table 5; standard deviations are given in Table 6. Statistical comparisons of gross weights recorded at each bridge based on the means and standard deviations indicated that the populations of 2D, 2S-2, and 3S-2 trucks and the combined values differed significantly at the 95 percent confidence level between the 2 sites. The comparisons were based on the assumption of a normal distribution, although the magnitude of the standard deviation relative to that of the mean indicates that the distributions may, in fact, be slightly skewed. The statistical difference is probably due to the fact that the large populations defined the mean quite accurately; the practical effect of differences between the 2 sets of data is considered insignificant.

The data indicate the relative importance from a design viewpoint of the 3S-2 truck because (a) it has significantly heavier axle and gross weights and (b) it is the most prominent combination, accounting for more than 50 percent of the total truck population in each case. The average axle spacings of the heavy 3S-2 truck are generally similar to those of the other 3-axle combinations.

DISCUSSION OF RESULTS

The stresses recorded in the beams of the 2 instrumented spans were quite low, and both structures are considered safe against fatigue failure. There is little reason to doubt the accuracy of the experimental data. The magnitudes of the stresses were verified theoretically, and the results of the I-95 study were similar to those obtained in a previous study (1). The magnitudes of the strain ranges recorded in the midspan diaphragm and the deck reinforcement of the I-95 bridge are not considered problematical.

The question of increasing allowable weight limits for trucks naturally arises, in light of the low stresses recorded in both structures. The authors did not recommend such an increase on the basis of this limited study of 2 structures. The test bridges both were of recent construction and both were designed to accommodate the heavy AASHO HS20-44 loading. They cannot be considered typical of many of the older bridges in Virginia. A recommendation concerning either increasing truck weight limits or modifying established design procedures would be more appropriate when more information has been developed in the nationwide program of loading history studies.

An interesting aspect of this study was the sensitivity of the beams to the pattern of service loads. It is, of course, expected that the beams under the load are the most highly stressed, and this fact, coupled with the tendency of truck drivers to remain in the right lane when traffic permits, results in more stress occurrences in the beams under the right lanes and many less occurrences in the other beams. Future studies could concentrate on those critical beams, using more gauges at selected points of a single member.

The theoretical analysis developed in this study served to verify the magnitudes of the experimental stress ranges. Although the correlation obtained between the number of stress events predicted by theory and that recorded in the field was less than perfect, the results are considered encouraging. Refinements to account for the effects of dynamic loading will be needed, and those may be developed in the broad program of loading history studies. The development of a theoretical means of assessing the service life of bridges is a goal of the national program.

CONCLUSIONS

The following conclusions are warranted by the results of this study:

1. The low strain ranges measured in both of the structures included in this study indicate that fatigue will not be a problem in either case under current truck load limits;
2. Stress ranges of a magnitude comparable to that in the main supporting elements were recorded in the midspan diaphragm of the steel beam span, and higher (but not critically high) stress ranges were recorded in the deck reinforcement of the span; and
3. The sensitivity of a typical bridge structure to the position of an applied load, coupled with the tendency of truck drivers to remain in the right lanes whenever possible, would allow the critical beam in a structure to be determined in many cases, and future studies could concentrate gauges on that structural element.

REFERENCES

1. Galambos, C. F., and Armstrong, W. L. Acquisition of Loading History Data on Highway Bridges. Public Roads, Vol. 35, No. 8, June 1969, U.S. Department of Transportation, pp. 177-189.
2. Galambos, C. F., and Heins, C. P., Jr. Loading History of Highway Bridges: Comparison of Stress Range Histograms. Highway Research Record 354, 1971, pp. 1-12.
3. Average Daily Traffic Volumes on Interstate, Arterial, and Primary Routes. Virginia Department of Highways, 1968, 1969, and 1970.
4. Report of Weighing Operations, December 31, 1970, Thirty-One Years. Traffic and Planning Division, Virginia Department of Highways, Richmond, Jan. 1971.
5. Highway Laws of Virginia. Reprinted from Code of Virginia and the 1970 Cumulative Supplement, Virginia Department of Highways.
6. ACI Standard Building Code for Reinforced Concrete, A.C. 318-63. American Concrete Institute, Detroit, 1963, Sec. 1102.

COMPARISON OF MEASURED AND COMPUTED ULTIMATE STRENGTHS OF FOUR HIGHWAY BRIDGES

Edwin G. Burdette and David W. Goodpasture, Department of Civil Engineering, University of Tennessee

Four deck girder highway bridges in Tennessee, located in an area to be flooded as a part of a TVA reservoir, were tested to failure under static loading. The ultimate load for each bridge, defined as the maximum load-carrying capacity of the bridge, was measured. This measured load was compared to loads that were computed by strain compatibility relations in which actual stress-strain properties of the materials were used and the entire bridge including curbs was assumed to act as a wide beam spanning between supports, and by the 1971 Interim Specifications of AASHO, in which the capacities of all girders were summed. In both methods, a flexural mode of failure was assumed. Also, the load causing first permanent set was computed and compared with the measured load. The analytical method based on strain compatibility predicted the ultimate capacity of 3 of the bridges within 9 percent. Each bridge failed in a flexural mode. Composite action was lost in the prestressed concrete bridge prior to flexural failure, with a resulting reduced load capacity. The loads based on AASHO Specifications gave a lower bound to the actual ultimate loads for each bridge. The load causing first permanent set is less readily identifiable, either theoretically or experimentally, than is the ultimate load. The method given in the AASHO Specifications for limiting overload on the basis of first permanent set appears reasonable.

•FOUR deck girder highway bridges, located in Franklin County, Tennessee, were tested to failure during the summer of 1970. These bridges were located in an area that has since been flooded as a part of the Tennessee Valley Authority's Tims Ford Reservoir and were made available by the Tennessee Highway Department and TVA for testing purposes. The testing was performed as a part of a research contract between the Civil Engineering Department of the University of Tennessee and the Tennessee Department of Highways in cooperation with the Federal Highway Administration. A complete description of the testing program and a compilation of the test results are given in the final report for the research project (1).

The apparent trend in the Specifications of the American Association of State Highway Officials is toward the use of "load factor design" for deck girder bridges. This design philosophy is based on the prediction of ultimate capacity of the individual bridge girders along with considerations of the amount of overload that would cause first permanent set and fatigue considerations. The research reported in this paper represents a unique opportunity to assess, through tests on typical highway bridges, the accuracy with which the bridge designer is able to predict ultimate bridge capacity and load causing first permanent set.

The primary objective of this paper is to compare the computed and measured ultimate strengths of each of the 4 bridges. Two values of computed ultimate capacity were obtained for each bridge: (a) The ultimate bridge capacity was determined by summing the ultimate capacities of each longitudinal girder in the bridge, as calculated on the basis of the 1971 Interim Specifications of AASHO (2); and (b) the capacity of each bridge was calculated on the basis of strain compatibility relations, using the actual stress-strain relations of the material in the structure. In the latter method the entire bridge, with curbs, was considered to act as a unit. In both methods, ultimate capacity was assumed to be controlled by the flexural strength of the bridges.

A secondary objective is to compare the theoretically calculated load causing first permanent set for each bridge with the value obtained from experimental load-deflection curves for the bridge. The behavior and mode of failure of each bridge, as observed in the tests, are described and discussed.

DESCRIPTION OF BRIDGES

Each of the four bridges was a 2-lane deck girder bridge with 4 longitudinal girders. A description of the bridges is given in Table 1, and photographs of the bridges are shown in Figure 1.

From a testing viewpoint, bridges 1 and 4 were the most useful of the 4 bridges. Bridge 1 was on a flat sag vertical curve; in all other respects these 2 bridges were ideal for testing: 90-deg skew, horizontal tangent, almost 0 grade, and recent construction.

Bridge 2, composed of AASHO type 3 precast, prestressed sections, was also of recent design and was a widely used type. Its usefulness as a test specimen, however, was limited somewhat by the presence of a 70-deg skew, a grade of approximately 4½ percent, and a superelevated roadway because of a 4½-deg horizontal curve. Although bridge 3 was not of recent design and had a 60-deg skew, it had a 0 grade and was not curved. Also, the reinforced concrete T-beam construction is representative of a number of bridges currently in use throughout the United States.

COMPUTATIONS

The ultimate load-carrying capacity of a bridge subjected to flexural loading depends not only on its own flexural capacity but also on the position of the applied loads. The position of the loads in the actual tests to failure is described in detail at a later point in this paper. For the tests, the loads were placed in such a way as to simulate an HS loading in the position resulting in maximum positive moment near the center of a span. It was that load position for each bridge that was used in the calculations to predict ultimate load-carrying capacity. The loads were assumed, for calculation purposes, to have uniform lateral distribution; that is, the loads were treated as line loads extending across the bridge deck.

All values given for maximum load-carrying capacity refer to applied live load. The moment due to dead load was subtracted from the total moment capacity prior to calculation of maximum load.

Theoretical Ultimate Capacity

The ultimate load capacity of each bridge was calculated on the basis of strain compatibility relations that considered the actual stress-strain properties of the steel and ultimate compressive strength of the concrete in each bridge. The stress-strain curves are shown in Figure 2. The average ultimate compressive strength of the concrete in the bridge decks for each bridge, obtained from cores, is given in Table 2. The coefficients given in the ACI Code (3) were used to define the concrete stress block in compression.

In the determination of theoretical ultimate capacity, each bridge was assumed to act as a unit, with the curbs acting as an integral part of the unit. Any effect of handrails was neglected.

The method used to calculate the ultimate moment capacity at both positive and negative moment sections of bridge 4 and the negative moment sections of bridge 1 was simply that of multiplying the experimentally determined yield stress of the steel by the plastic modulus. The determination of ultimate moment capacity at positive moment sections in bridges 1, 2, and 3 involved consideration of both concrete and steel; the method used required the application of 3 necessary relationships: equilibrium of horizontal forces and moments, assumption of linear strain distribution, and knowledge of the stress-strain relations for concrete and steel. The method of analysis, particularly as applied to prestressed concrete beams, is described in detail elsewhere (4, 5).

Once the ultimate moment capacity was calculated for simple-span bridges 2 and 3, the determination of ultimate load consisted of calculating the applied load that, acting

Table 1. Description of bridges.

Number	General Description	Span (ft)	Girder Spacing		Skew (deg)	Location	Design Loading and Date
			Feet	Inches			
1	4-span continuous, 36-in. steel rolled beams, composite in positive moment regions	70, 90, 90, 70	8	4	90	Tenn-130 over Elk River	HS-20, 1963
2	Simple span composite with AASHO type 3 precast, prestressed concrete beams	66	8	10[a]	70	Tenn-130 over Boiling Fork Creek	HS-20, 1963
3	Simple span reinforced concrete T-beams, monolithic construction	50	6	10	60	US-41A over Elk River	H-15, 1938
4	3-span continuous, noncomposite, 27-in. steel rolled beams	45, 60, 45	7	4	90	Mansford Road over Elk River	H-15, 1956

[a]Varies because of 4½-deg horizontal curve.

Figure 1. Test bridges.

Bridge 1

Bridge 2

Bridge 3

Bridge 4

Table 2. Measured and computed results.

Bridge	Avg Ultimate Compressive Strength (psi)	Ultimate Load			Centerline Deflection (in.)	Load Causing First Permanent Set		
		Measured (kip)	Theoretical (kip)	AASHO (kip)		Measured (kip)	Computed (kip)	Permanent Deflection (in.)
1	6,800	1,250	1,270	930	22.8	620	714	0.25
2	5,500	1,140	1,267	1,100	9.5	660	759	0.12
3	6,500	1,580	1,465	844	7.2	—	—	—
4	5,600	640	696	388	26.4	500	376	0.00

in combination with the existing dead load, would produce the calculated ultimate moment. For continuous bridges 1 and 4, a "limit analysis" was made in which redistribution of moments after yielding was considered. Figure 3 shows the position of the applied loads on the loaded span for each bridge and the magnitudes of the calculated ultimate moments. The end moment at the pier at the left of the span for bridge 1 is that caused by dead load only, because there was no provision at the left abutment for resisting an upward reaction, and the load causing failure was large enough to cause the bridge to lift off the abutment. The theoretically calculated ultimate loads are given in Table 2.

Ultimate Capacity Predicted From AASHO Specifications

The 1971 Interim Specifications of AASHO (2) were used as a basis for calculation of the ultimate capacity of bridges 1, 2, and 4. These specifications do not provide for the determination of ultimate capacity of reinforced concrete bridges such as bridge 3. Thus, the AASHO Specifications' value of ultimate capacity for bridge 3 was calculated by using the general method presented for determination of flexural capacity in the ACI Code (3); this method is believed to hold to the "spirit" of the 1971 AASHO Interim Specifications. The ultimate loads calculated by the AASHO Specifications are given in Table 2.

Bridge 1—The concrete and steel properties for this bridge were taken as $f_c' = 6{,}000$ psi and ASTM A-36 respectively. The ultimate positive moment capacity near the center of the span, based on composite design, was calculated to be 13,600 kip-ft. This value was obtained by summing the flexural capacities of all 4 girders. The position of the loads was such that, when the ultimate moment was reached near the center of the span, the sections at the supports were still elastic. The Specifications make no provision for limit behavior; therefore, the maximum load was calculated as that which produced the ultimate moment near the center of the loaded span. A computer analysis of the structure was carried out through the use of ICES STRUDL-II and took account of the nonprismatic bridge cross section. The maximum load-carrying capacity was calculated on this basis to be 930 kips.

Bridge 2—The concrete and steel properties for this simple-span bridge were taken as $f_c' = 5{,}500$ psi and $f_s' = 250$ ksi respectively. The 4 AASHO-PCI type 3 precast girders were assumed to act compositely. The ultimate moment capacity for the entire bridge was calculated on the basis of the AASHO Specifications to be 17,400 kip-ft, and the maximum load-carrying capacity was calculated to be 1,100 kips.

Bridge 3—The concrete and reinforcing steel properties for this simple-span bridge were taken as $f_c' = 4{,}500$ psi (limited by AASHO Specifications, section 1.5.1B) and $f_y' = 40{,}000$ psi. The ultimate moment capacity was calculated to be 9,660 kip-ft, and the maximum load-carrying capacity, 844 kips.

Bridge 4—The steel in this noncomposite, 3-span continuous bridge was assumed to be A-36. The loads were placed on the span such that, when the plastic moment was reached near the center of the center span, the sections at the piers were still elastic. The total plastic moment for the bridge was calculated to be 3,500 kip-ft. The maximum load-carrying capacity was calculated, on the same basis as that described for bridge 1, to be 388 kips.

Calculation of Load Causing First Permanent Set

The 1971 AASHO Interim Specifications (2) attempt to ensure that permanent deformation will not occur under a specified overload by limiting the moment caused by dead load plus an amplified live load with impact to 95 percent of that causing first yield. For comparisons discussed later in this paper, the load producing first yield of the steel in bridges 1, 3, and 4 was calculated and is given in Table 2. The calculations were based on the experimentally determined yield strength of the steel in each bridge, and elastic theory was used.

Figure 2. Stress-strain curves for steel.

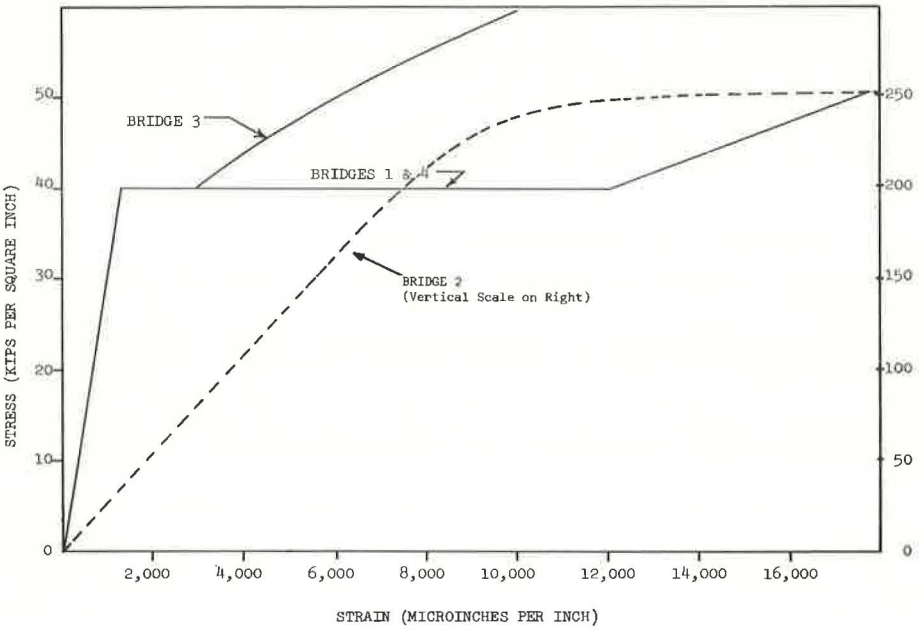

Figure 3. Location of applied loads and magnitudes of calculated ultimate moments (M* for bridge 1 = maximum moment that could be developed at first pier because of dead load only).

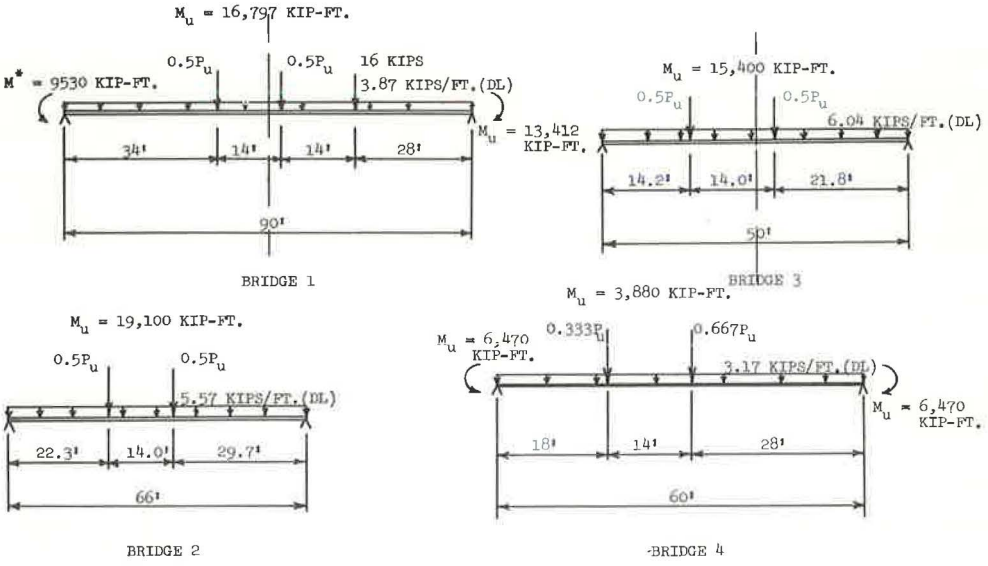

TEST PROCEDURE

Placement of Loads

The loads were placed on each bridge with the exception of bridge 4 in such a way as to simulate an HS truck located in each lane to cause maximum positive moment near the center of the span. The points on the span at which load was applied were at the positions of the 8 rear wheels of the 2 simulated trucks. For the test to failure of bridge 1, the 4 front wheels were simulated by four 4,000-lb pallets of concrete blocks. The simulation of front wheels was omitted for the other bridges. The positions of the applied loads for the 4 bridges are shown in Figure 4. Because of difficulties in rock drilling, only 6 load points were used for bridge 4.

Application of Load

The rather large loads required to cause bridge failure were developed through a "rock anchor system" and were applied to the bridge deck through a "bearing grill."

Rock Anchor System—At each of the 8 load points for each span, a hole was drilled through the concrete bridge deck. Directly below each one of these holes, a hole was drilled approximately 25 ft into the limestone rock, and an 18s reinforcing bar was grouted into place in this hole. The bar was terminated below the bridge deck, and a connection accommodating a $1\frac{3}{8}$-in. diameter Stressteel bar was welded to the top end of the 18s bar. After completion of all rolling load and other tests on each bridge, a $1\frac{3}{8}$-in. diameter Stressteel bar was connected to each of the 18s bars. The Stressteel bar extended through the hole in the bridge deck and through a 100-ton capacity center-hole jack, which rested on a bearing grill.

Bearing Grill—The bearing grill consisted of two 14-in. wide flange beams, 3 ft 10 in. long, spaced 2 ft 6 in. center-to-center. These beams were joined at the ends by two 12-in. channels, which spanned between the beams and were welded to the beams so that the bottom flanges of the channels were flush with the bottom surfaces of the beams in order to obtain uniform bearing. Two more channels spanned between the beams at the center of their 3-ft 10-in. length and were fastened to the beam webs. The load was applied by the hydraulic rams through a 2-in. thick steel bearing plate to these center channels. Soft wood two-by-tens were placed under the beams and on the bridge deck, and two-by-fours were placed under the end channels in order to minimize stress concentrations and reduce the likelihood of punching shear. In addition, it was necessary to cast concrete bearing pads on superelevated bridge 2 in order to apply the loads to a horizontal surface.

Loading Procedure

The load was applied to each load point by a Stressteel center-hole ram acting on a bearing grill. The rams were activated by an electric pump equipped with a pressure gauge that had a maximum capacity of 10,000 psi. The loads were applied in increments of 1,000 psi to near yielding and then in increments of 500 psi to failure. The force in each bar was obtained from strain readings after each increment of load. Also, strains at various points in the bridge were monitored, and level rod readings at several points on the bridge deck were taken after each load increment. The tests were discontinued at some point after the ultimate load of the bridges was attained. Ultimate load is defined as the maximum load attained in a test to failure, and failure is said to have occurred when an increase in deflection of the bridge takes place under a decreasing load.

TEST RESULTS

Behavior Mode of Failure

Each of the 4 bridges, with the exception of bridge 2, failed in a flexural mode, and each bridge behaved in a ductile manner. Load-deflection curves for one point near the centerline of the span on each bridge are shown in Figure 5; modes of failure are shown in Figure 6.

Figure 4. Position of loads used in tests.

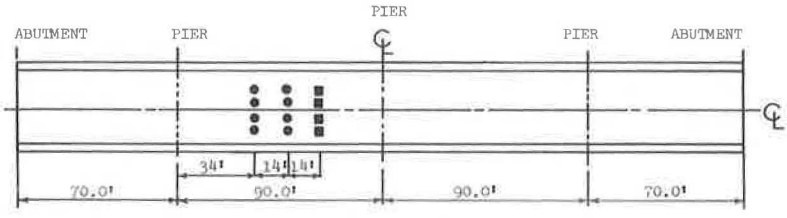

BRIDGE 1

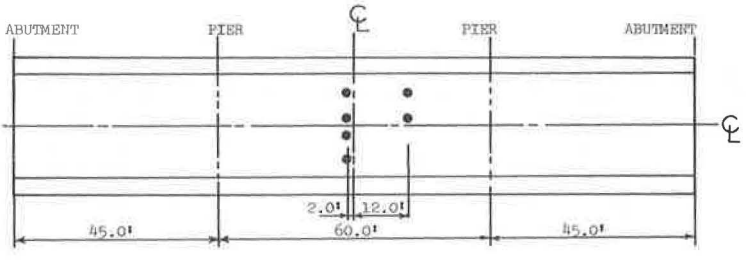

BRIDGE 4

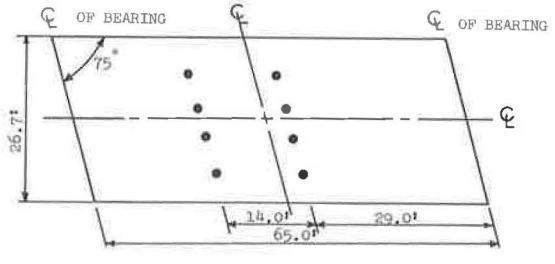

BRIDGE 2

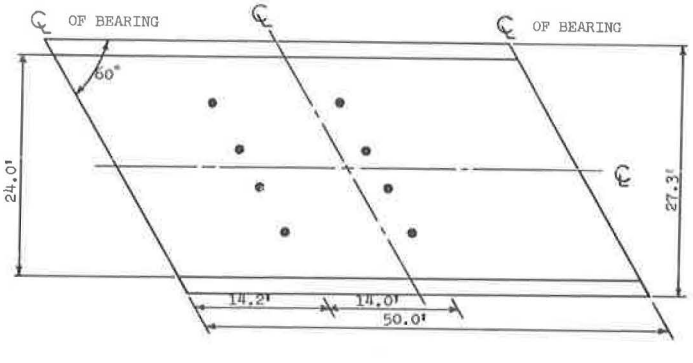

BRIDGE 3

● LOAD POINT

■ 4 KIP LOAD

Figure 5. Load-deflection curves.

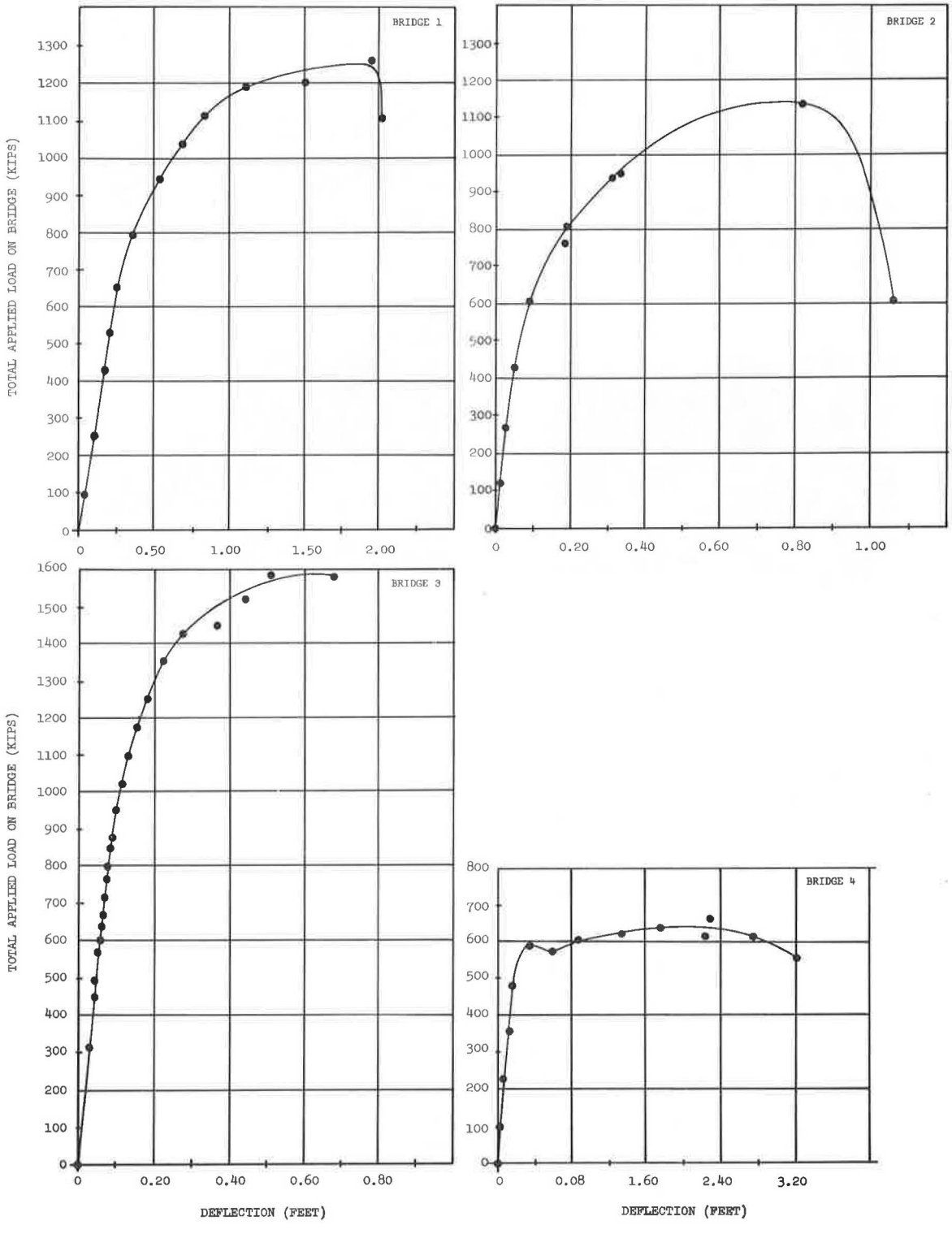

Figure 6. Mode of failure.

Bridge 1

Bridge 2

Bridge 4

Figure 7. Measured and computed ultimate loads.

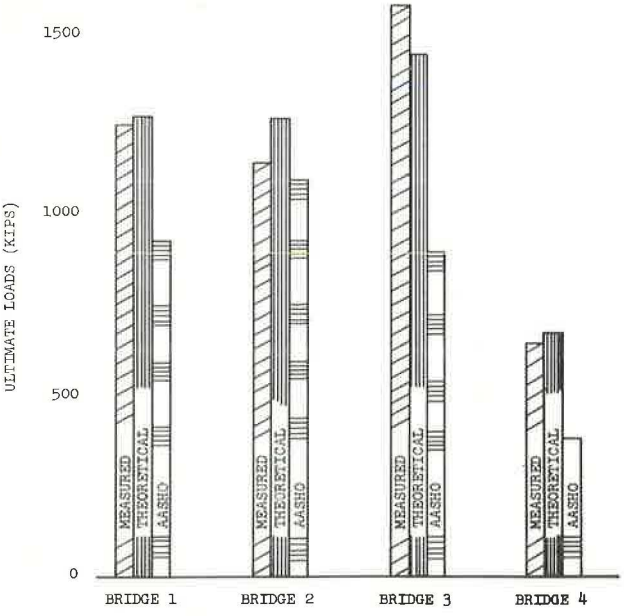

Bridge 1—The behavior of this bridge was almost linearly elastic up to yielding at the section under the applied loads nearest the center of the span. As the load was increased, there was considerable rotation at this section and, in turn, considerable deflection. Shortly after yielding began and the load was increased further, the bridge "lifted off" the abutment nearest the applied load, thus making it impossible to develop more moment at the first pier. The bridge continued to experience increasingly large deflections for each load increment until, after a very large deflection, yielding occurred, and a plastic hinge formed at a section near the center pier at the end of the cover plates on the side of the pier away from the loaded span. Shortly after this hinge formed, a secondary compression failure of one of the curbs occurred at the section of maximum positive moment, and the test was terminated.

Bridge 2—This bridge behaved in a predictable way up to a load of approximately 950 kips. However, there was considerable "dishing" of the bridge at this point, and the interior girders were deflected considerably more than the exterior girders. The result of this dishing was a tendency for the bridge deck to separate from the interior precast girders. At a load of approximately 950 kips this separation occurred, and composite action of the interior girders was lost as the vertical stirrups crossing the interface between girder and deck were sheared. After composite action was lost, the behavior of the bridge was radically changed. Almost immediately there was crushing of the extreme top fibers of the interior precast sections at the section of maximum moment. This crushing and accompanying rotation resulted in a redistribution of moments at the section and an increase in the moment in the exterior girders. As the load was increased further, the interior girders failed in shear, and the test was terminated.

Bridge 3—This bridge, designed in 1937 for the equivalent of an H-15 loading, had the highest capacity of any of the other bridges tested. It behaved elastically up to very high loads, and it was not obvious when yielding first occurred. The reason for the absence of a clearly defined yield load is related to the stress-strain curve for the steel (Fig. 2), which indicates a very short yield plateau. Yielding did not occur simultaneously in all steel bars in all members at a cross section. The strain in the most highly stressed bars would increase to the strain-hardening region while other bars were reaching yield. This continuing process resulted in the behavior shown in Figure 5.

Bridge 4—The load-deflection curve for this bridge closely resembles that for a typical intermediate grade of structural steel, which is not surprising in view of the fact that the bridge was a noncomposite steel girder type. The stiffness of the bridge up to yield was considerably greater than that predicted for a noncomposite bridge because partial composite action existed up to yield. Failure of the bridge was initiated by yielding at the section of maximum positive moment. After this occurrence there followed considerable rotation of the resulting plastic hinge and very large deflections with only a nominal increase in load. Then plastic hinges formed near the 2 piers on the sides away from the loaded center span, and further deflection took place with a reduction in load capacity.

Ultimate Loads

The ultimate loads obtained from the field tests and the centerline deflection at ultimate load are given in Table 2.

COMPARISON OF RESULTS

Ultimate Loads

A comparison of calculated and measured ultimate loads is shown in Figure 7.

Theoretical Method—For all bridges except bridge 2 the theoretical method described earlier predicted within 9 percent the ultimate capacity of each bridge. The value predicted for bridge 2 was significantly higher than the measured value because of the loss of composite action in the interior girders at a load less than ultimate. The mode of failure for each bridge, again with the exception of bridge 2, was the same as that predicted. Redistribution of moments occurred in continuous bridges 1 and 4, and a limit analysis predicted the ultimate capacity very closely. The fact that the predicted ca-

pacity of bridge 4 was some 9 percent larger than the actual capacity was due, probably, to the eccentric placement of loads. This placement resulted in a rather uneven lateral distribution of load, with the likelihood that all 4 girders were unable to attain their maximum moment capacities simultaneously.

AASHO Specifications—The ultimate loads predicted by the AASHO Specifications were, in all cases, less than those measured. For bridges 1 and 4 the reason for the relatively low value predicted by AASHO Specifications is the fact that no redistribution of moments at ultimate load was considered. The ultimate load was calculated as that which produced ultimate moment at the section of maximum moment. The reason that the ultimate load calculated by using AASHO Specifications for bridge 3 was much lower than the measured value is due, most likely, to the fact that the maximum steel stress was taken as that at yield. Actually, because of the short yield plateau for the steel and the fact that a low percentage of steel was used, the steel stress at ultimate was much above yield.

Load at First Permanent Set

The load causing first permanent deflection set is not a clearly defined quantity, from either a theoretical or an experimental viewpoint. The computed values for this load were based on first yielding of steel. The measured values were taken from load-deflection curves for each bridge, and the load selected was that at which there was a definite deviation from a straight line. Computed and measured values for bridges 1, 3, and 4 are given in Table 2. No attempt was made to identify this load for prestressed concrete bridge 2. The computed loads for bridges 1 and 3 are somewhat higher than the load taken from load-deflection curves; however, the measured permanent deflection at a load equal to the computed load was approximately $\frac{1}{4}$ in. for bridge 1 and $\frac{1}{8}$ in. for bridge 3. Thus, the computed load causing first permanent set can be considered reasonable. The computed load for bridge 4 was approximately 75 percent of the measured load. This difference is most likely due to the fact that some degree of composite action did exist up to first yield, and the computations were based on the noncomposite behavior of the bridge.

CONCLUSIONS

The comparison of computed and experimentally determined results presented in this paper permits the following conclusions to be drawn:

1. The ultimate capacity of each bridge was computed on the basis of using material properties experimentally determined, considering an entire bridge to act as a wide beam spanning between supports, using a strain-compatibility method to determine ultimate moments, and taking account of redistribution of moments in continuous bridges 1 and 4. The ultimate capacities calculated in this manner agreed quite closely with the values obtained through field testing. The close agreement indicated that, as the load on a bridge is increased beyond first yielding, the more heavily loaded interior girders begin to yield, and additional load is taken by the exterior girders. Finally, near ultimate load, each girder is stressed approximately to its ultimate capacity, and the total bridge capacity approaches that obtained by considering the bridge to act as a wide beam, with the entire cross section including curbs acting as an integral unit.
2. The ultimate capacity of each bridge was also calculated on the basis of AASHO Specifications; specified nominal values for steel strengths were used. The loads obtained in this manner did not compare as closely with the actual ultimate bridge capacities as those calculated by the more exact method described earlier. However, design use of the more exact method is impractical. Thus, it is important to note that the calculations based on AASHO Specifications give a lower bound to the actual ultimate capacity of each of the 4 bridges tested.
3. The definition and experimental determination are somewhat less clear for load causing first permanent set than for ultimate load capacity. However, it appears from the tests and calculations that the method given in the AASHO Specifications for limiting overload on the basis of first permanent set is reasonable.

ACKNOWLEDGMENTS

Appreciation is expressed to the Tennessee Department of Highways for help in numerous ways during the conducting of the research described in this paper. Also, appreciation is expressed to the Tennessee Valley Authority for consistent cooperation. Finally, the advice, encouragement, and assistance given by Robert Varney and his co-workers at the Federal Highway Administration are gratefully acknowledged. The opinions, findings, and conclusions expressed in this paper are those of the authors and not necessarily those of the state or the Federal Highway Administration.

REFERENCES

1. Burdette, E. G., and Goodpasture, D. W. Final Report for Full-Scale Bridge Testing. Submitted to Tennessee Department of Highways and Federal Highway Administration, Dec. 31, 1971.
2. 1971 Interim Specifications. Committee on Bridges and Structures, American Association of State Highway Officials.
3. Building Code Requirements for Reinforced Concrete. American Concrete Institute, ACI 318-63.
4. Warwaruk, J., Sozen, M. A., and Siess, C. P. Investigation of Prestressed Reinforced Concrete for Highway Bridges: Part III—Strength and Behavior in Flexure of Prestressed Concrete Beams. Eng. Exp. Station, Univ. of Illinois, Bull. 464, 1962.
5. Khachaturian, N., and Gurfinkel, G. Prestressed Concrete, McGraw-Hill, 1969.

STRUCTURAL BEHAVIOR OF THE SOUTH ROAD CURVED GIRDER BRIDGE

Robert F. Victor, Bureau of Highways, Connecticut Department of Transportation

Presented are the major results of a field study that included the field testing of a horizontally curved, steel-girder bridge of welded I-girder and concrete slab construction and the subsequent analyses made to determine the analytical stresses and deformations that would match those produced by the construction and test vehicle static loadings. Analyses were made with the approximate and curved grid methods with variations in the stiffness parameters of moments of inertia and torsional constants. A comparison with slab-load experimental data revealed that the dead-load flexural stresses and vertical deflections could be predicted by both methods. Dead-load response was found to be relatively independent both of the torisonal constants of the girder members and of the transverse stiffness of the structure (moments of inertia of diaphragms and slab). The live-load tests were conducted with an FHWA test vehicle that was driven along 5 different lanes. The approximate method could not predict flexural stresses or vertical deflections, nor could either method be made to give lateral bending stresses. Rotations could not be predicted by the grid method. Other effects investigated were nonlinear stresses due to wheel contact and web slenderness.

•WITH EMPHASIS in recent years on structures of clean, aesthetically pleasing lines and surfaces, horizontally curved girders have increasingly been used for structures on difficult curved alignment. Two factors tending to increase their use have been the subjugation of bridge alignment considerations to roadway alignment considerations and the increased span lengths of overpass structures over divided highways, resulting from the elimination of side piers for traffic safety. When the overpassing roadways have moderate to sharp curvature, continuous spans for the bridge structures would be ruled out and simple spans with their greater girder depths and large slab overhangs would be required unless continuous curved girders were utilized.

In spite of the increased number of curved bridges built in the past few years and the various analytical methods advanced to explain their behavior (1, 2, 3, 4, 5), the stress distribution in a structure with horizontally curved, welded I-girders remains the subject of conjecture; and thus improvements to these methods await the investigation of the structural behavior of various curved girder bridges.

In the design of any bridge, it is desirable to know the stresses and deflections that occur in any part of the structure so that plate dimensions of girders can be held to a minimum consistent with permissible stresses and deflections. Realistically, any analytical method used in practice must employ simplifications and approximations so that design times can be shortened. Any improvements in the analytical methods must satisfy the criteria of significant improvement in economy or improvements in structural performance or both.

It is to this last statement that this paper is addressed. Would the knowledge of the structural response of a full-scale curved girder bridge to dead and live loads be of use in establishing criteria to improve analytical methods used in curved-girder design? This paper is concerned with the interpretation of data from a program of dead- and live-load testing and a comparison of these data with two analytical methods, the "approximate method" (3, 6) and a curved grid program (2) currently used by the Bridge Design Section of the Connecticut Department of Transportation. It is hoped that the

information presented here will contribute to a better understanding of the structural behavior and help to determine criteria for the design of curved-girder bridges.

EXPERIMENTAL BRIDGE

Designed by Edward F. Hubert of the Connecticut Department of Transportation, the South Road grade separation is the first curved-girder bridge in Connecticut. Carrying a 2-lane local road over Interstate 84 in Farmington (Fig. 1), the structure has a 40-ft roadway with a centerline radius of 1,043 ft and is 2-span continuous (175 ft each on centerline South Road).

In cross section (Fig. 2), the bridge has 3 steel girders 19.25 ft on centers. The girders vary in depth from 7 ft at midspan to 12 ft at the pier. Cross frames are 17.5 ft on centers, at the tenth-points of the span, and are in the form of K-bracing with a separate top chord member (Fig. 2). Lateral bracing frames in at every other cross-frame connection (Fig. 3). The detailed girder data are shown in Figure 4. The reinforced concrete deck is haunched over the girders with a $9\frac{1}{2}$-in. minimum thickness between girders. Details of sidewalk, parapet, wearing surface, and protective fencing are shown in Figure 2.

The structure was designed as noncomposite by using the approximate method of analysis (3, 6) to determine the stresses in the girders and to proportion plate sizes accordingly. A 3-girder system was selected principally for fabrication economy; substructure units were set radially. Girder depths were set somewhat deeper than the minimum permitted of L/25 (7) to offset the expected increased deflection of the outside girder and to provide a greater overall rigidity.

SCOPE

The girders were instrumented at 3 sections along the bridge for both the dead- and live-load testing. Four cross frames had strain gauges for the dead-load testing; for the live-load testing, only 2 cross frames had gauges (Fig. 5).

Deflections were observed in the dead-load testing (Fig. 6) at 3 points on each girder in each span. Points in one span are symmetrical to those in the other. Deflections and bottom-flange rotations for the live-load testing were obtained at locations shown in Figure 5. The location of the pair of deflection gauges at section 7, girder 1, is symmetrical to that of section 9, girder 1. Girder 1 had more deflection gauges so that a determination could be made of its deflected shape under load.

The loads for the dead-load testing consisted of formwork, slab, wearing surface, sidewalk, and parapets. Because of the many problems encountered and the inconsistencies in the results of this testing, all but a small portion of the slab-load results were disregarded (8). The latter experimental stresses are compared to those produced by the approximate method (3) and a curved grid analysis (2).

The live load was an FHWA test vehicle that closely simulated an HS20 truck. Both static-position and crawl-run data were obtained by oscillograph recordings. However, because the static-position test results are somewhat unreliable because of drift, the crawl-run test data were developed more fully and were used almost exclusively for comparison with analytical values. Live-load responses investigated are as follows:

1. The variation of flexural and lateral bending stresses with location of the FHWA test vehicle,
2. The vertical deflections and torsional rotations of the bottom flanges with the passage of the test vehicle,
3. The stresses in the bottom angles of a pair of cross frames,
4. The variation of the distribution of moment among the 3 girders at a midspan cross section for the different lateral positions of the test vehicle,
5. The effect of stiffnesses of the various structural components (slab, cross frames, and girders) on the stress distribution in the structure, and
6. Localized secondary stress effects adjacent to the wheels of the test vehicle.

Figure 1. General bridge views.

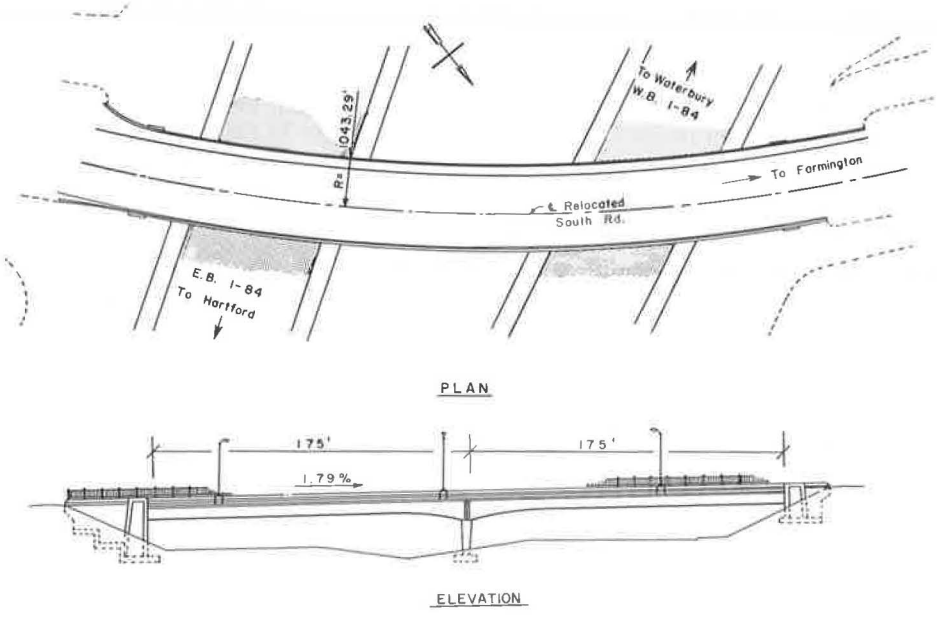

Figure 2. Typical bridge cross section.

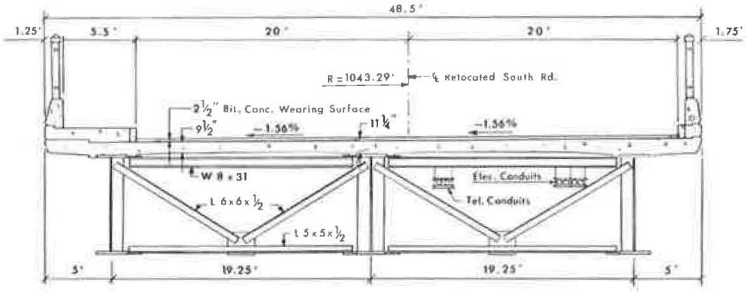

Figure 3. Half-framing plan (north span shown).

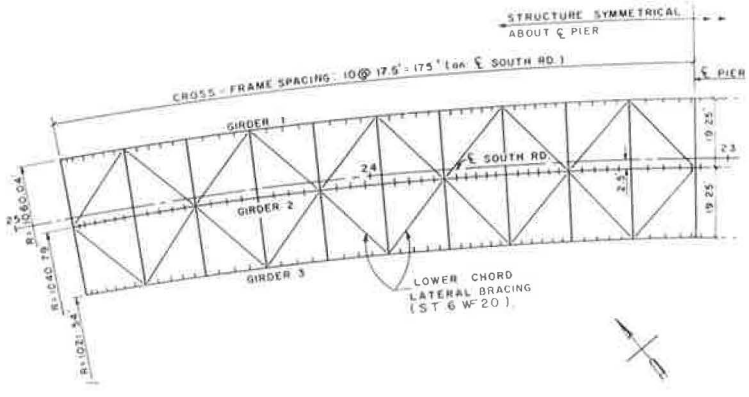

Figure 4. Girder data.

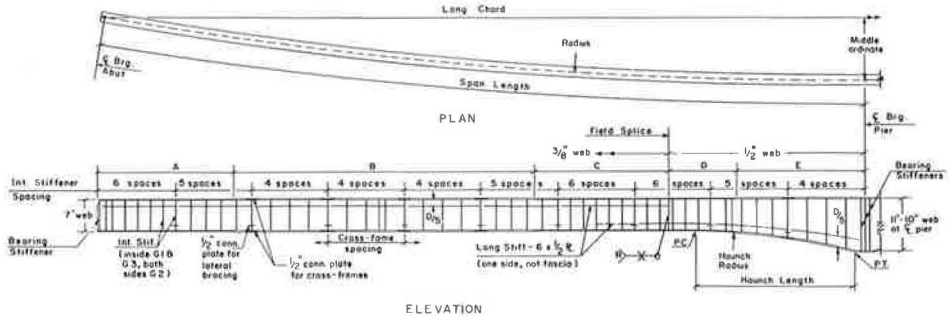

Girder	Span Length	Radius	Middle Ord.	Haunch Length	Haunch Radius	ASTM Des.	A Flange	A Length	B Flange	B Length	C Flange	C Length	ASTM Des.	D Flange	D Length	E Flange	E Length	C-Frame Spacing	Stiffeners Int.	Stiffeners Bearing
1	177.81	1060.04	14.88	40.00	167.93	A441M	30x1 5/8	31.00	30x2 1/16	70.00	30x1 3/8	31.00	A441M	30x1 3/8	16.00	30x2 1/8	29.81	17.78	10x 3/8	14x1 1/4
2	174.58	1040.79	14.61	39.00	159.76	A441M	28x1 1/2	30.75	28x2	68.50	28x1 1/8	30.75	A441M	28x1 1/8	15.50	28x2 1/4	29.08	17.46	8x 1/2	13x1 1/8
3	171.35	1021.54	14.34	38.00	151.80	A36	26x1 3/4	25.50	26x2 1/16	76.50	26x1 1/8	25.50	A441M	26x1 1/8	17.00	26x2 1/8	26.85	17.14	10x 5/8	12x1 1/8

Note: Since design is non-composite, top and bottom flanges are the same.
Haunch Radius is to bottom of web.
Plate dimensions are in inches. Other dimensions are in feet.

Figure 5. Plan of grid model with gauge locations.

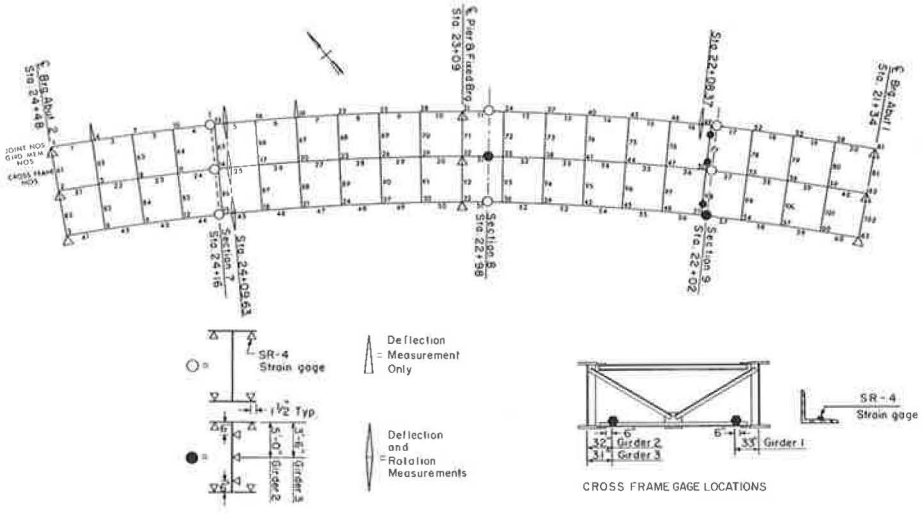

Figure 6. Slab pour sequence.

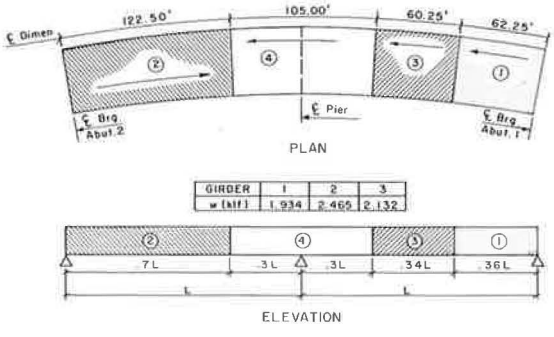

ANALYTICAL COMPARISON AND DISCUSSION OF DEAD LOAD

The purpose of the dead-load testing was to experimentally determine the stresses and deflections due to each increment of loading and to determine whether the analytical methods used in design would predict these stresses and deflections. If these stresses and deflections could not be determined with the parameters used in design, then what adjustments would be required to match the analytical values to the experimental?

Because of the experimental procedures followed, however, the dead-load data obtained are marginal (8). Although the experimental total stress is not known, the incremental loading stresses of slab pours 2, 3, and 4 were considered sufficiently accurate for comparison with analytical values.

Analytical Methods

The approximate method of analysis was originally proposed in a U.S. Steel Corporation report (3), and its use, with modifications, is illustrated in a U.S. Steel handbook (6). The following procedure was used in the analysis for each slab pour:

Each girder was analyzed (by using a plane frame computer program) as a straight 2-span continuous girder using the developed member lengths. Primary moments (6) were obtained by using the loads shown in Figure 6 for the load lengths indicated. Joints in the girder were located at cross-frame intersections so that moments could be compiled directly from output in order to facilitate computing V-loads, the shear loads induced on the inner and outer girders by torsion (6). In general, V-loads act downward in positive moment areas and upward in negative moment areas on girders outside the centerline of the girder system. For girders inside the centerline, the opposite is true.

For a 3-girder system, the V-loads are both equal and opposite for inner and outer girder. These loads are then input along with the slab loads to obtain the final shears, moments, and deflections of girders 1 and 3.

At this point, a lateral bending analysis is made of the flanges using the lateral-force magnitudes, M/R, at the cross-frame locations. The lateral force used in the analysis has an assumed straight-line variation from one cross frame to the next, and the computer program uses a reduced stiffness matrix (just the slope-deflection coefficients for rotations) to determine the lateral-bending moments.

The grid method was derived from and uses (with modifications) the stiffness equations for curved beams reported by Lavelle and Boick (2). For analysis, the structure is reduced to a gridwork of one-dimensional prismatic members consisting of curved grid members and diaphragm members that may be idealized as beams or trusses (5). The grid is analyzed by a standard analysis procedure termed the stiffness or equilibrium method. The method uses the slope-deflection coefficients for bending stiffnesses of a member and a torsional stiffness coefficient for twisting of a member. The member stiffness matrices thus formed are then transformed from the member-oriented axes to the structure-oriented axes by rotation matrices. The upper-band portion of the structure stiffness matrix is then generated preparatory to solution by Cholesky's square root method.

The computer program used for analysis generates structure geometry from input of the parameters of girder radii, span lengths, and diaphragm spacing. Members are then assigned properties of moments of inertia and torsional constants. Solution of equations (described earlier) is obtained by use of the Cholesky square root method that gives the structure displacements due to an applied loading. The displacements are then used to obtain the member end actions (shear, torque, and moment) for each member.

The flexural stresses were then obtained by hand calculation. The moments, shears, and applied loading from a lateral bending analysis (using girder torques instead of M/R quantities) were used to obtain, also by hand calculation, the lateral bending stresses at the gauge locations.

Flexural Stresses

The dead-load stresses were compared for slab pours 2, 3, and 4 at various gauge locations. Agreement with computed stresses was in many cases poor when gauges

had drifted appreciably between pours. For gauges that remained relatively stable, results were generally better. More intensively examined were girder 2 at section 8 and girder 3 at section 9. Those gauge locations had strain gauges on the web and could give a better idea of stress distribution. The results are shown in Figures 7 and 8. Figure 7 shows that approximate, grid, and experimental stresses agree fairly well. The top-flange stresses for pours 2 and 3 are out of line with the other two but in these cases the top flange was exposed to heating by sunlight. When the top flange was finally covered in pour 4, that effect did not exist. No stresses can be presented for the lower half of the girder at this location because those gauges were inoperative. In all cases noncomposite section properties were used because the analytical stresses and deflections would generally be less than the experimental if partial composite action from previous pours is taken into account.

Figure 8 shows that results are less certain because the gauge at the center of the web had drifted badly and was unreliable (along with the top-flange gauges). Stresses from pour 4 were too small to be measured. The stress distribution shown in Figure 8 is based on the assumption that the strain gauges involved did not drift appreciably from the previous pour. Where the concrete is over the gauge location, the top-flange stress drops to less than that of the top-web gauge. This effect could be caused by shear lag in the wide flanges (9, 10); however, more gauges on the top flange would be needed to verify this effect. Consistent departure from straight-line stress variation across narrow flanges has been observed in other bridges (11) without apparent explanation.

Vertical Deflections

Figure 9 shows girder deflections for the total of all pours; Figure 10 shows girder deflections for slab pour 2. Similar results were obtained for pours 1, 3, and 4 but pour 2 gives the largest deflections.

Comparing analytical with experimental deflections shows some unusual results. For the relatively "clean" (i.e., the least effects from partial composite action) structure of slab pour 2, the analytical values are consistent with those of the experimental. Figure 9 (the total slab load deflection) shows that the deflected shape of the structure is the sum of construction deflections rather than the total load applied to a weightless elastic structure. The greater total deflections in the north span would seem to be a result of partial composite action of slab pour 2 that prevented the equaling of deflections in both spans.

In attempting to reproduce the various experimental dead-load deflections with the grid program, we used various combinations of properties: noncomposite, noncomposite with transverse slab stiffness, and composite analyses. Inclusion of transverse slab stiffness is simply adding the section properties of the slab to those of the cross frames. The torsion constant for a composite section was computed as $\Sigma(\frac{1}{3}bt^3)/n$. Inclusion of transverse slab stiffness decreased the maximum deflection by 4 percent; inclusion of composite action reduced the noncomposite maximum deflection by 28 percent. However, the composite analysis produced deflections that were too small in comparison to those measured. Of interest also is the fact that in this structure the diaphragms are cross frames. If these cross frames are idealized as trusses instead of beams, the end actions should be different for a given set of unit deformations (member stiffnesses) (5), thus conceivably changing the structure response. However, this modification changed little. As found in live-load analysis, the structure response is highly insensitive to changes in transverse stiffness.

Also found is the fact that the response of this structure is very insensitive to the torsional constant. Torsional constants used ranged from approximately 200 in.^{4} ($\Sigma\frac{1}{3}bt^3$) to 90,000 in.^{4} for girder members. Negligible variation was noted in analytical response (8).

Lateral-Bending Stresses

Only some general observations can be made about lateral-bending stresses because experimental values were inconclusive. In all cases, experimental stresses were greater in magnitude than predicted. Interaction of formwork and top flanges is not

Figure 7. Dead-load stress distribution at section 8, girder 2.

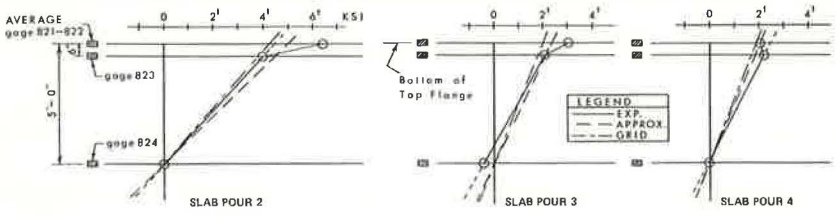

Figure 8. Dead-load stress distribution at section 9, girder 3.

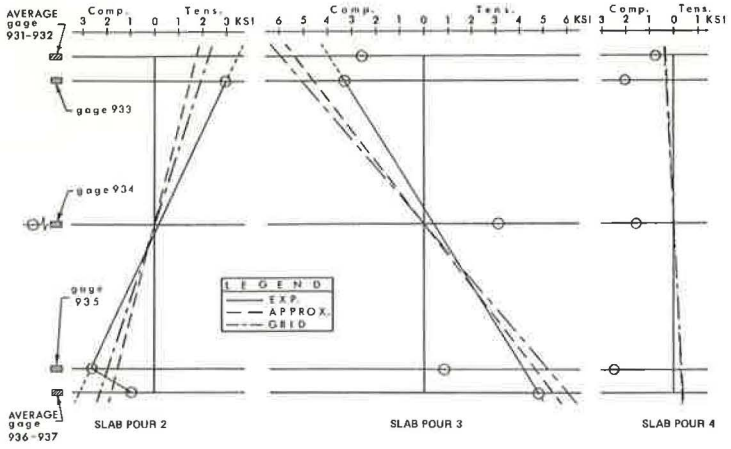

Figure 9. Total slab load deflection.

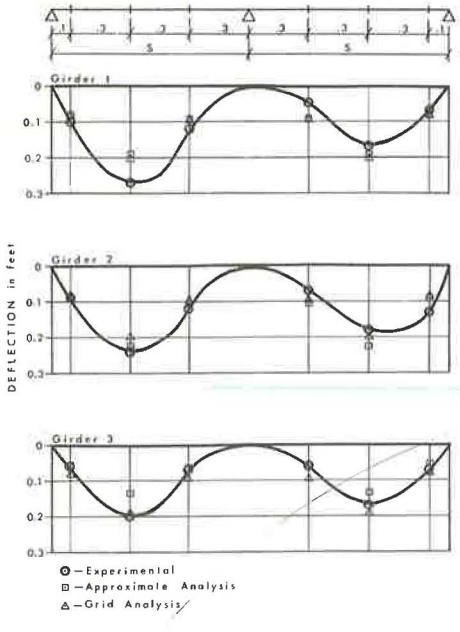

Figure 10. Pour 2 slab load deflection.

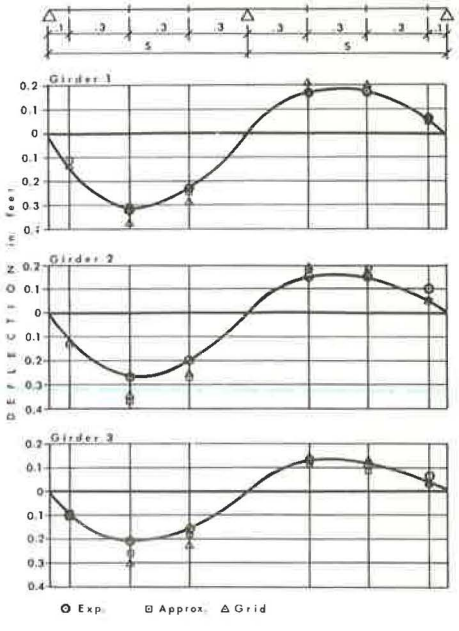

known but might have some effect because it laterally restrains the top flanges. With a series of slab pours, the top flange is unable to bend laterally under the hardened concrete slab; therefore, lateral-bending stresses under this slab should be zero for future loadings. Thus, these conditions of lateral restraint would seem to invalidate the lateral-bending analysis for reproducing experimental stresses.

ANALYTICAL COMPARISON AND DISCUSSION OF LIVE LOAD

Analytical Methods

The approximate method used for live-load analysis is nearly identical to that used for the dead-load analysis. Because the grid method was used as the main tool of analysis, the approximate method was confined to the noncomposite (the design basis) and the completely composite cases. No lateral-bending analysis was done in conjunction with this method. The method of applying the wheel loads of the test vehicle to the structure was the same for both the approximate and the grid methods. Wheel loads were distributed on a simple-span basis to adjacent joints (the intersections of girders and diaphragms).

The grid method is basically that described for dead-load analysis. Many different combinations of section properties were used in trying to reproduce experimental response. Composite sections used varied the parameters of modular ratio and slab widths. Torsional constants were computed as $\Sigma \frac{1}{3}bt^3$ until the entire width of slab with parapets was used. Torsional constants were then increased arbitrarily until experimental vertical deflections were matched. Transverse slab stiffness was tried both with and without the cross frames as diaphragm members.

The basic grid program was altered to increment the test vehicle along the structure in each of the lanes and to output the resulting stresses at the gauge locations (including lateral-bending stresses). Each position constitutes an alignment of front axle with diaphragm line. Diaphragm lines are numbered as their intersection with girder 1 (Fig. 5). Thus, for example, position 3-16 means lane 3, front axle at diaphragm members 66 and 87 (Fig. 5).

As data reduction proceeded, experimental results were compared to noncomposite grid analyses. From the resulting deflections and stresses, it was evident that more stiffness and strength would be needed to match the experimental results. Various composite sections were used: first, with AASHO criteria (7); second, with full slab width, modular ratio reduced to 5, parapets and sidewalk included in section properties of girders 1 and 3, and complete composite action included in the negative moment area; third, with torsional constant increased to 60,000 in.^{4} for each girder member; and, fourth, with preceding torsional constant changed to 90,000 in.^{4}.

Stress Distribution

The live-load stress distribution in the positive moment areas is basically linear with some small variation especially from web to flange (Fig. 11). In general, stress distribution across a moderately wide flange of a welded girder is nonlinear (9, 10, 11). Hence, for the flange gauge positions chosen, the measured stresses would not necessarily line up with those in the web.

In the negative moment area, the stress distribution in each girder is nonlinear because of the deep web (Fig. 12), the greater portion of which is in compression. This nonlinearity not only is caused by the truck itself but exists because the web is initially deformed from welding vertical stiffeners and has laterally deflected from the dead load. Only one longitudinal stiffener was used in this location. A more linear stress distribution would probably result from the use of multiple stiffeners.

Figure 12 shows, for truck position 3-37, that there is no readily discernible stress distribution. This stress pattern (or lack of it) is always true when the truck's wheels are nearby (see also the stress distribution shown in Fig. 13). The flexure formula, Mc/I, does not appear to govern under the influence of contact stresses imposed by the concentrated wheel loads (12). Indeed, the greatest top-flange stress occurred when the wheels passed by the gauge location. For all locations, these top-flange stresses

Figure 11. Live-load stress distribution at section 9, girder 3.

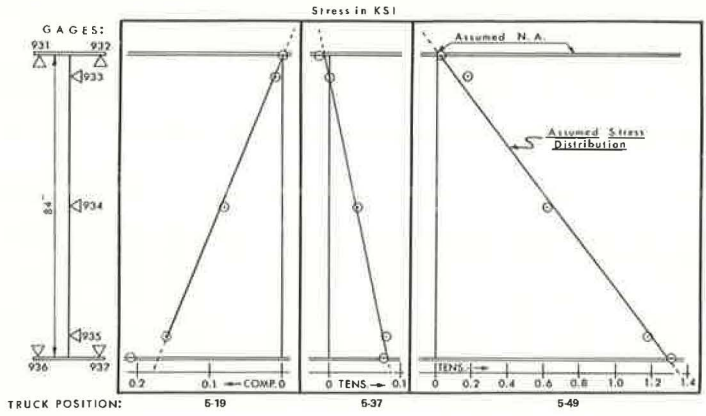

Figure 12. Live-load stress distribution at section 8, girder 2.

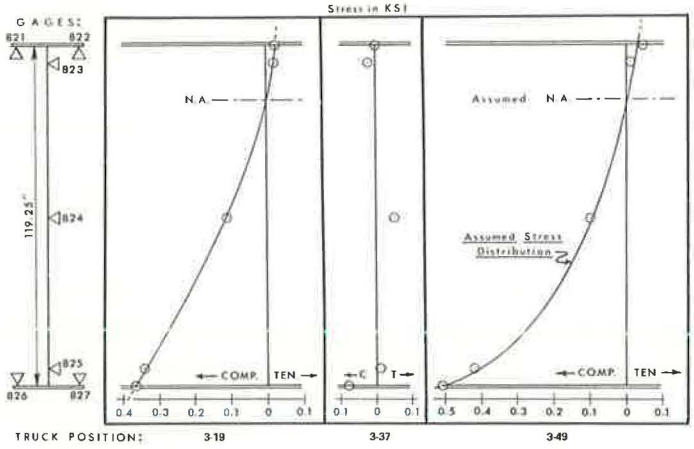

Figure 13. Typical stress behavior near wheels.

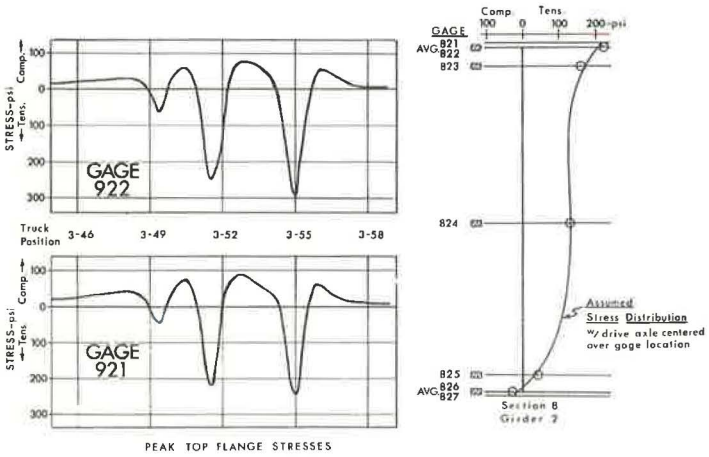

were always tensile. Figure 13 shows a typical top-flange gauge response. As the truck approaches the gauge location, there is a rise in the compressive stress; however, as the axle passes over the gauge location, there is a pronounced stress reversal. For truck position 3-55, a curved stress distribution is obtained with the neutral axis near the top of the slab for section 8, girder 2.

Neutral Axes and Modular Ratios

Apart from those truck locations where contact stresses dominated, neutral axes locations were generally at or near the top flange of the girder in all gauge locations. At section 9, girder 3, the neutral axis was finally assumed to be at the top of the top flange (because some small shifting of the neutral axis was noticed for various truck positions). For calculating a neutral axis location in the positive moment area, the following is needed: a modular ratio of 5; a slab width determined from the midpoints between the girders; for girder 1, inclusion of a portion of the parapet below the top of curb; and, for girder 3, inclusion of the sidewalk and the portion of parapet below the top of sidewalk. The top portion of the parapet was finally disregarded because it brought the neutral axes up too high. The parapets have vertical joints that are from 18 to 19 ft apart and are used to control shrinkage cracking. These vertical joints nullify the stiffening effect that the parapets otherwise might have.

A modular ratio of 5, used in the positive moment areas, is that which results from using the initial tangent modulus (based on the average 28-day cylinder strength of 5,200 psi). With the low stresses, rapid loading, and slab reinforcement, a modulus of elasticity of the slab or 5,800 ksi (n = 5) is certainly possible. In the negative moment area, the neutral axis at section 8, girder 2, was assumed to be about 19 in. below the bottom of the top flange (Fig. 12). If a modular ratio of 8 is assumed for the slab in tension, the computed neutral axis will be in the above location. Also if the reinforcing steel is considered separately from the concrete in computation for neutral axis location, a modular ratio of 9 is required for the concrete alone. With the low stresses encountered, we might logically expect to have the same modular ratio for both tension and compression because we are using the initial tangent modulus. However, the cracking of the concrete under shrinkage and permanent tensile stresses would account for this discontinuity in the slope of the stress-strain relation. With shrinkage cracking evident on the underside of the deck and under future repeated live-load action, the modular ratio in the tensile area should increase with time until perhaps the reinforcing steel acts alone. Composite action from the wearing surface was not considered.

Concrete Stresses

The concrete stresses from the three gauges were at all times very small. In comparing strains from the gauges on the bottom of the haunch with those on the adjacent top flange, we found that these strains were compatible. This compatibility would indicate complete, rather than partial, composite action.

Cross-Frame Stresses

The stresses produced by the readings from the cross-frame gauges show that these members are very active in the response of the structure. The maximum stresses produced were equal to those of the girder bottom-flange gauges (2 ksi maximum) and were found to be quite sensitive to the lateral position of the test vehicle.

If we consider the vertical deflections and rotations at section 7 to be representative of those at this particular cross frame, we find the bending stresses from analysis as a rigid frame to be very small under the maximum deformations. Thus, the stresses due to axial forces should predominate. With the gauges installed as shown in Figure 5, it is not possible to separate axial from bending stresses. Again when the measured vertical and rotational deformations from section 7 are used, it is apparent that the experimental stresses are consistent with the relative vertical deflections and especially the relative lateral deflections of the bottom flanges (the bottom flange rotations being

used as a measure of lateral deflection) of the adjacent girders. The lateral deflections of the girders were not measured and could not be found from measured rotations.

Rotations

The rotations were measured on the bottom flange, which in general is not the average rotation of the girder. Because of the flexibility of the web, the bottom-flange rotations will be different from those of the slab. The bottom-flange rotations were found to be greater than the chord rotations of the slab (the relative girder deflections divided by the spacing) for girders 1 and 3 and less for girder 2. Generally, with the increasing torsional constants from the different grid analyses, the rotations decreased to the order of the experimental but in no way matched those values.

Vertical Deflections

With the increase in moments of inertia and torsional constants, the vertical deflections decreased noticeably for all girders, in proceeding from the noncomposite to completely composite analysis. With the increase in torsional constant to 90,000 in.^{4} for each girder member, the deflections matched the experimental results from the gauges in the north span with the truck in that span (Figs. 14, 15, and 16). With the truck in the north span, the predicted vertical deflection for the deflectometer pair near section 9, girder 1, was consistently high (always an upward deflection). This predicted response was too high because a modular ratio of 5 was assumed in the negative moment area, but the neutral axis location at section 8, girder 2, shows that n = 8 with full slab width. Therefore, the area near the pier (negative moment area) is less stiff than assumed in analysis. If this reduced stiffness is used, all the predicted vertical deflections should match the experimental. Thus, the following parameters are needed for member properties in order to match analytical grid deflections to the measured values:

1. The full width of the slab;
2. An initial tangent modulus of elasticity for the modular ratio in the positive moment area (slab always in longitudinal compression);
3. A reduced modular ratio in the negative moment area (slab always in longitudinal tension) to account for transverse cracking;
4. A torsional constant of approximately 90,000 in.^{4} for each girder member; and
5. Diaphragm stiffnesses with a moment of inertia of the slab equal to that calculated by $bh^3/12n$, taking the width of slab equal to the cross-frame spacing and the thickness equal to the minimum slab thickness and adding the moment of inertia of the cross frame computed as $\Sigma A\bar{y}^2$ of the top and bottom horizontal members (this approach works because the response of this structure is grossly insensitive to the variation in transverse stiffness).

Girder Stresses

The flange flexural stresses, measured as the average from the 2 flange gauges, were closely approximated by the grid method analysis, which matched the computed with the experimental deflections. Generally, for this particular analysis, computed stresses are higher than the experimental for bottom-flange stresses. If changes were made to the section properties as suggested for vertical deflections, these changes would be beneficial for comparing bottom-flange stresses because neutral axes would drop somewhat and lower the stresses. The changes in moments would be relatively small because moments are more insensitive to property changes than are the structure deflections and stresses.

Top-Flange Stresses

Flexural stresses were either zero or very small at sections 7 and 9 because the neutral axes are close to the top flanges at these sections. The lateral-bending stresses were always zero at all sections (any recorded difference was of the order of the

Figure 14. Girder behavior at section 7, lane 1.

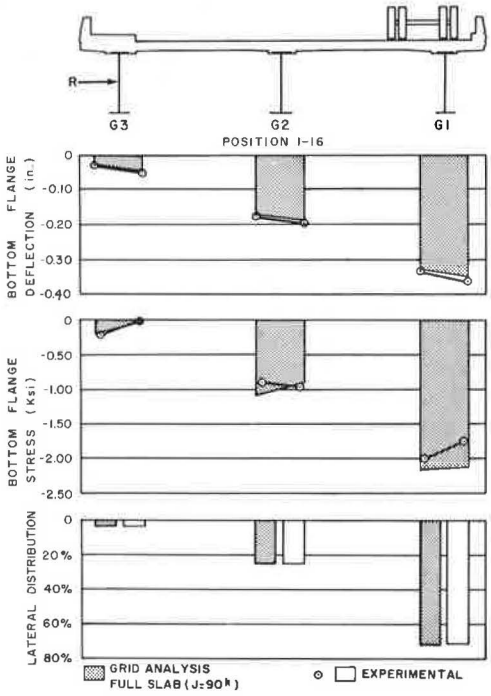

Figure 15. Girder behavior at section 7, lane 3.

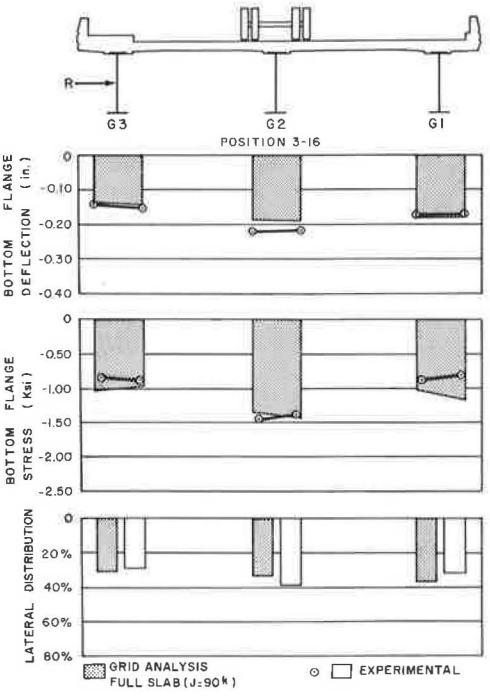

Figure 16. Girder behavior at section 7, lane 5.

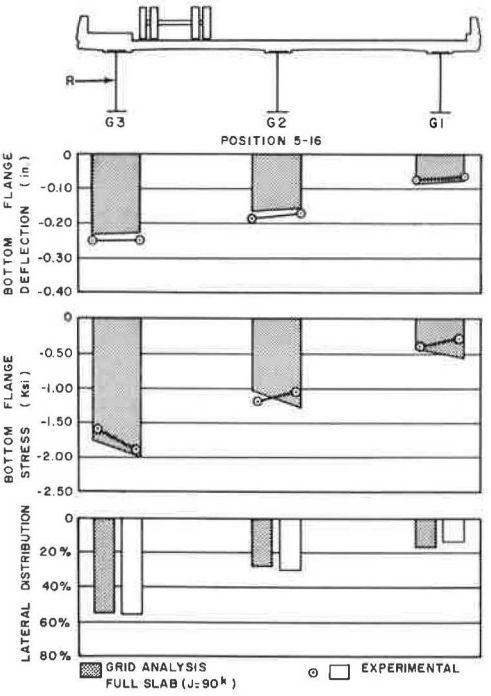

gauge accuracy) because the slab is infinitely stiff in its own plane (4). Most interesting is the variation in top-flange stresses when the wheels of the truck pass by the gauge location (Fig. 13). There is a complete live-load stress reversal at sections 7 and 9 and an increase in tensile stress at section 8. These stresses do not change the sign of the total stress in the top flanges (the dead-load stress is much larger) but, because of the compatibility of strain between the concrete and steel, the slab undergoes the stress reversal in the longitudinal direction. This reversal of stress with a moving truck would be very quick and more than likely contribute to the deterioration of the slab.

Bottom-Flange Stresses

The bottom-flange flexural stresses were consistently approached by the grid method as the stiffness parameters were increased to match the experimental vertical deflections with those of the grid analyses. The lateral-bending stresses were not approached by use of the girder torques in combination with the method in the U. S. Steel publications (3, 6). Other approaches for determining lateral-bending stresses seem too complex for design (13, 14), or the assumption of either total or zero torsional restraint at the ends of a member (15) is questionable. The most promising of the methods investigated for determining lateral bending stresses was that of Bouwkamp and Powell (11) in which the bottom flanges and web are represented as additional grid members. Thus, lateral-bending stresses can be computed from the member end moments on the bottom-flange members from this type of grid analysis.

Distribution Coefficients

Experimental distribution coefficients were determined by multiplying the average bottom-flange stress by the computed section modulus (which gives the experimental moment) and then by taking each moment as a percentage of the total moment at the test cross section. Results are shown for 3 lateral positions for the moments at section 7 in Figures 14, 15, and 16.

In obtaining the lateral distribution percentages, we found that the total moment at the cross section did not vary with the lateral position of the test vehicle. For each of the truck positions 1-16, 3-16, and 5-16 the total moment at section 7 was approximately 1,963 ft-kips. From the grid analysis, the total moment was 2,200 ft-kips. Use of section properties, which excluded the parapets, gave a total moment of 1,996 ft-kips.

Concluding Discussion

Throughout the live-load analysis, alterations were made to member properties in the grid method. This method was used as the main tool of analysis because it is a more sophisticated analytical tool than the approximate method. Although the approximate method with noncomposite section properties was used for design, it was found that it could not match the experimental live-load stresses and deflections. A distribution of the test vehicle's wheel loads to the joints (the intersections of girders and diaphragms) was done on a simple-span basis for all analyses. This initial distribution proved to be adequate for the grid method because this method is able to further distribute the applied loading. The total moment at the cross section is the same for both approximate and curved grid methods. Thus, the problem is one of lateral distribution of moment and deflection, and it would appear that an initial distribution of wheel loads, other than on a simple-span basis, is needed if the approximate method is to give valid flexural stresses and vertical deflections. With the grid method, the correct lateral distribution of moment and deflection was achieved by simply increasing the torsional constant.

The live-load vertical deflections and flexural stresses (and by implication, lateral distribution of moment) were matched to the experimental with the curved grid method. Torsional rotations were approached, but bottom-flange, lateral-bending stresses were not matched because these stresses are more closely related to the effects of nonuniform torsion. The approximate method, while giving the correct longitudinal distribution of moment, did not give a valid lateral distribution.

As a final analysis, the structure was assumed to be straight. It was found that the variation in response was at most 10 percent with most responses showing less variation. Thus, it may be said that the effect of curvature, for this structure, is to increase the stresses and deflections by not more than 10 percent.

REFERENCES

1. McManus, P. F., Nasir, G. A., and Culver, C. G. Horizontally Curved Girders—State of the Art. Proc. ASCE, Vol. 95, No. ST5, May 1969, p. 853.
2. Lavelle, F. H., and Boick, J. S. A Program to Analyze Curved Girder Bridges. Division of Engineering, Research, and Development, Univ. of Rhode Island, Kingston, Eng. Bull. 8, 1965.
3. Gordon Richardson and Associates. Analysis and Design of Horizontally Curved Steel Bridge Girders. U.S. Steel Corp., Struct. Rept., 1963.
4. Ketchek, K. Another Approach to Simplified Design of a Curved Steel Girder. AISC Eng. Jour., Vol. 6, No. 4, Oct. 1969.
5. Weissman, H. A. Straight-Element Grid Analysis of Horizontally Curved Beams. AISC Eng. Jour., Vol. 7, No. 2, April 1970.
6. Highway Structures Design Handbook. Vol. 1, Ch. 12, U.S. Steel Corp.
7. Standard Specifications for Highway Bridges. American Association of State Highway Officials, Washington, D.C., 1969.
8. Victor, R. F. Structural Behavior of the South Road Curved Girder Bridge. Bureau of Highways, Connecticut Department of Transportation, March 1971.
9. Beedle, L. S., et al. Structural Steel Design. Ronald Press Co., New York, 1964.
10. Bresler, B., and Lin, T. Y. Design of Steel Structures. John Wiley and Sons, New York, 1960.
11. Bouwkamp, J. G., and Powell, G. H. Structural Behavior of an Orthotropic Steel Deck Bridge. Department of Civil Eng., Univ. of California, Berkeley, Rept. SESM-67-27, 1967.
12. Seely, F. B., and Smith, J. O. Advanced Mechanics of Materials. John Wiley and Sons, New York, 1952.
13. Heins, C. P., Jr., and Seaburg, P. A. Torsion Analysis of Rolled Steel Sections. Bethlehem Steel Co., Steel Design File 13-A-1, 1964.
14. McManus, P. F., and Culver, C. G. Nonuniform Torsion of Composite Beams. Proc. ASCE, Vol. 95, No. ST6, June 1969, p. 1233.
15. Lyse, I., and Johnston, B. G. Structural Beams in Torsion. Trans., ASCE, Vol. 101, 1936, p. 857.

CLOSING REMARKS AT SYMPOSIUM ON BRIDGES: LOADING HISTORY, ULTIMATE STRENGTHS, AND PERFORMANCE

Charles F. Galambos, Federal Highway Administration,
U.S. Department of Transportation

•THE ONE recurring theme from all of the papers presented at the symposium was that measured stresses were small and well below the live-load design stresses, and that therefore, there is no need to be concerned about fatigue problems in highway bridges. For the great majority of bridges, that statement is true. There have been very few reported instances of traffic-induced fatigue problems in the main load-carrying members of bridges.

However, the recent discovery of several cracked beams on a relatively young bridge (12 years of service) on the Connecticut Turnpike has raised the question of how relevant these other bridge-loading history tests are to the very high-volume, heavy-truck arteries in the congested urban areas of the country. Some observers believe that it will only be a very short time before fatigue cracking on certain bridges will be a major repair problem.

It is urged, therefore, that extensive loading history tests be made on the bridges in these high-traffic urban areas and that the owners of the bridges make especially close inspections of those details likely to suffer fatigue damage. It may well be that there is more fatigue damage than has been heretofore recognized, or publicly admitted. In this connection, it is strongly urged that there be established a more open line of communication between bridge maintenance engineers and the bridge design and research community. Very little is learned from hidden failures.

The paper by Heins and Khosa presents a method for relating truck gross weights to induced girder stresses and is a step in the right direction. Admittedly, the method is approximate and empirical, based on only a small sample of field tests, but it is simple; for the cases considered it is probably as accurate as the usual variations encountered in fatigue testing. The method should be verified for other traffic, bridge, and span conditions.

SPONSORSHIP OF THIS RECORD

GROUP 2—DESIGN AND CONSTRUCTION OF TRANSPORTATION FACILITIES
John L. Beaton, California Division of Highways, chairman

Committee on Dynamics and Field Testing of Bridges
Robert F. Varney, Federal Highway Administration, chairman
James W. Baldwin, Jr., Edwin G. Burdette, Michael E. Fiore, Charles F. Galambos, Egbert R. Hardesty, Conrad P. Heins, Jr., Cornie L. Hulsbos, Henry L. Kinnier, Kenneth H. Lenzen, W. H. Munse, Leroy T. Dehler, W. W. Sanders, Jr., Chester P. Siess, William H. Walker, Robert K. L. Wen, G. W. Zuurbier

L. F. Spaine, Highway Research Board staff